Abstracting and indexing

Journal is indexed in Crossref, İndex Copernicus, Scilit and E-library

Azerbaijan Journal of Chemical News

Contacts
Address: 20 Azadliq av., Baku, AZ1010, Azerbaijan,
Phone: +994124986533,
Email:minira.agahuseynova@asoiu.edu.az, mayaabdullayeva@asoiu,edu,az,
ali.alizada.q@asoiu.edu.az, rena06.72@yandex.ru

ASOIU
Azerbaijan State Oil and Industry

CONTENT

ASOIU
Azerbaijan State Oil and Industry

AJCN, Vol .7, No.2 , 2025, pp.4-17
https://doi.org/10.32010/AJCN04022025-4

ISOTHERM ADSORPTION STUDIES OF Cd (II) ION REMOVAL FROM AQUEOUS SOLUTIONS BY MODIFIED RUBBER-BASED ADSORBENT

[1]*Israfil Movsumzada*[0009-0005-6457-1552]
Department of Chemistry and chemical engineering
Researcher of Nanotechnology laboratory, Khazar University
movsumovisrafil@gmail.com
[2]*Tahir Javadzade*[0009-0008-8587-1361]
Department of Chemistry and chemical engineering
Lecturer, PhD, Khazar University
tjavadzade@khazar.org
[3]*Khalilova Fergana*[0009-0009-4974-6683]
Department of Analytical chemistry
Lecturer, PhD, Baku State University
ferqana_28@mail.ru
[4]*Famil Chiragov* [0000-0002-2677-9046]
Department of Analytical Chemistry
Professor, doctor of chemical sciences, Baku State University
ciraqov@mail.ru

Abstract: *This work is dedicated to adsorption study of Cd (II) ions by 1-[1-Methyl-2-(methylamino) ethyl] thiourea modified synthetic rubber. The impact of pH, contact time, initial metal ion concentration were among the several parameters influencing the adsorption process that was studied throughout the research. The highest adsorption capacity was achieved with 593.47 mg/g at pH=3 after modification with new thiourea derivative. Five adsorption isotherm models were examined to explain the adsorption process, and it was found that results are in agreement with the Redlich–Peterson Isotherm. The Temkin model was examined and found that there is chemical adsorption occurs in the adsorbent-adsorbate system. Desorption study are also included in this paper to study regeneration property of the adsorbent. So, 0.5 mol/l H_3PO_4 has demonstrated the maximum desorption capability over Cd (II) ions.*
Keywords: *adsorption, Cd (II), modification, isotherm, modification, thiourea.*

INTRODUCTION

Water is a vital natural resource required for the existence of all living species and the proper functioning of ecosystems [1,2]. However, growing urbanization, expansion of industry, and agricultural intensification have caused extensive pollution of water bodies across the world. Heavy metals are particularly concerning among contaminants due to their non-biodegradability and severe toxicity at extremely low doses [3]. Cadmium is a major representative of this group element since it is both non-essential and hazardous [4].

The high toxicity and bioaccumulation potential of cadmium make it one of the most hazardous heavy metals [5]. Despite being extremely rare (0.1–0.5 ppm) in the Earth's crust, cadmium is frequently released into the environment by human activities such the smelting of copper, lead, and zinc [6]. Additionally, it is commonly used in industrial processes including electroplating, the manufacturing of pigments and plastics, PVC stabilizers, phosphate fertilizers, nickel-cadmium batteries, and other alloys [7]. The main sources of cadmium contamination in surface and groundwater are

wastewater discharges from these businesses and improper disposal of objects containing cadmium [8]. Because of its high environmental persistence and ability to pass through food chains, cadmium can have long-term ecological and biological consequences [9].

Cadmium has no recognized physiological use in the human body, in contrast to several other metals that are useful as trace elements. Rather, even at very low quantities, it is very hazardous [8]. Inhaling industrial pollutants, consuming tainted food, or drinking water can all expose one to cadmium [10]. The buildup of this substance in the body mostly impacts the kidneys [11], liver [12] and bones [13], resulting in skeletal deterioration [14], hepatotoxicity [15], and nephrotoxicity [16]. Prolonged exposure is linked to reproductive damage [17], cardiovascular disorders [18], pulmonary dysfunction [19], and an elevated risk of cancer [20]. Clinical symptoms include bone softening [21], joint pain [22], respiratory distress [23], anemia [24], hypertension [25], and gastrointestinal disorders [26]. Owing to its high toxicity, the World Health Organization (WHO) has set the maximum permissible limit of cadmium in drinking water at only 0.003 mg/L, reflecting its potential threat to human health even at trace levels [27].

Given its persistence, toxicity, and widespread occurrence, cadmium removal from aqueous environments has become an urgent research priority in ecological and analytical chemistry [28]. Traditional treatment methods, such as chemical precipitation, ion exchange, membrane filtration, and electrochemical techniques have a number of disadvantages, including high operational costs, incomplete removal at low concentrations, and secondary waste generation [29]. In comparison, adsorption has emerged as one of the most efficient, cost-effective, and versatile methods for cadmium remediation. This technique offers simplicity, high efficiency at trace levels, reusability of adsorbents, and adaptability to large-scale applications[30].

Recent advances in materials science have focused on the development of novel adsorbents with enhanced affinity and selectivity for cadmium ions [31]. Among them, functionalized polymers and polymer-based composites have gained increasing attention due to their stability, tunable chemical properties, and potential for modification with active functional groups [32,33].

The present study aims to investigate the adsorption behavior of Cd (II) ions from aqueous solutions using a specially designed resin-based sorbent and it was modified with a thiourea derivative to improve its sorption capacity. The research focuses on evaluating the effects of pH, contact time, ionic strength, and initial metal ion concentration. In addition, desorption studies were performed to identify suitable regenerating agents. All studies was done in both static and dynamic conditions. To gain a better understanding of the sorption process, theoretical calculations were also done.

EXPERIMENTAL PART

Devices

The optical densities of the solutions were measured with a BK-UV 1600 Biobase spectrophotometer. The pH values of the solutions were measured using PHS-3DW digital pH meter. Distilled water was obtained through Biobase (WD-A10) water distiller device. The dynamic experiments were leaded by using SK-O180-Pro Digital Orbital Shaker.

ISNN: print 2663-7006; online 2709-2666

Preparation of solutions

The stock solution of cadmium (10^{-2} M) was prepared by dissolving appropriate amount of $Cd(NO_3)_2 \times 4\ H_2O$ in 100 ml of distilled water. The equilibrium concentrations of Cd (II) ions in the solution were determined with the help of the xylenol orange (R).

Buffer solutions with pH values ranging from 3 to 8 were prepared by mixing appropriate proportions of 0.1 M acetic acid (CH_3COOH) and ammonium hydroxide ($NH_3 \times H_2O$) and for pH 2, a hydrochloric acid (HCl) solution was employed as the acidic medium.

All the reagents that used were analytical grade pure.

Synthesis and identification of sorbent

For the experiment, we have used already synthesized rubber and for modification the novel thiourea derivative, the synthesis carried out according to the literature [34].

Synthesis of 1-[1-Methyl-2-(methylamino)ethyl]thiourea

The synthesis of N-substituted thiourea derivative was performed according to the literature [34,35].

For the reaction 1-(methylamino) propan-2-ol and thiourea were taken in the same mol ratio with 0.1 mol. So, a three-necked flask is filled with 10.3 g of 1-(methylamino)propan-2-ol and 7.6 g of thiourea then 10 ml of trifluoroacetic acid is added while stirring quickly, then the liquid is heated to 40–50^0 C for completely dissolve the thiourea. The stirring is ceased after four to five hours. Distillation is used to eliminate the trifluoroacetic acid. A water pump is used to remove the organic material from the solution. Precipitation in methyl alcohol yields 72% of 1-[1-methyl-2-(methylamino)ethyl]-thiourea.

Table 1

Summary of analysis results

Name	Structure	Brutto formula	Element Analsis	Spectral analysis	
1-[1-Methyl-2-(methylamino)ethyl] thiourea	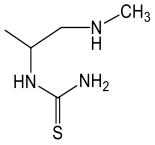	$C_5H_{13}N_3S$	C 40.82%, H 8.84%, N 28.57%, S 21.77%.	NMR	^{1}H NMR (300 MHz, $CDCl_3$, δ, ppm): 9.53 (s, 2H, NH_2), 7.31 (s, ^{1}H, NH), 2.47 (d, 3H, CH_3), 2.0 (m, ^{1}H, NH), 2.64–2.89 (t, 2H, CH_2), 3.03 (d, ^{1}H, CH), 1.13 (s, 3H, CH_3). 13C NMR (75 MHz, $CDCl_3$, δ, ppm): 18.6, 53.3, 57.6, 36.2, 184.7.
				IR	$\nu(NH_2)$ = 665, 711, 742, 847, 878 sm^{-1}, $\nu(R_2NH)$ = 1562 sm^{-1}, ν (CH_2) = 2925, 2855, 1462 sm^{-1}, ν(C=S) = 1129, 1168, 1243, 1313, 1365, 1377 sm^{-1}, ν (CH_3) = 1462, 1377 sm^{-1}.

As it is seen from the table 1, all desired functional groups are found in new thiourea derivative.We could predict from this data that the metal will be strongly bounded with this functional groups based on previous theoretical and experimental analysis.

Sorption experiments

Batch sorption experiments for Cd (II) were carried out at ambient temperature (25 ºC). In each run, 2 mL 5 × 10^{-3} mol·L^{-1} concentration of cadmium solution was transferred into 100 mL glass reagent bottle with screw cap. Subsequently, 30 mg of the sorbent was added and the pH of the suspension was adjusted to the desired value. The mixtures were left for 24 h to attain equilibrium, then the solid phase was separated from the aqueous phase by using filter paper. Dynamic sorption experiments were led by same order by using automatic orbital shaker.

The equilibrium concentration of metal ions in the solution was determined by known spectrophotometric method using xylenol orange as organic reagent (pH 6; λ=575 nm) [36].

The degree of sorption and removal percentage of metal ions are calculated by the following formulas:

$$R_{\%}=\frac{C_0-C_e}{C_e}100 \quad \text{(I)}$$

$$q_e=\frac{(C_0-C_e)V}{m} \quad \text{(II)}$$

Here, C_0 is the initial concentration of the metal ion (mol·L^{-1}), C_e is the equilibrium concentration of the metal ion (mol·L^{-1}), V is the volume of the solution (L), and m is the mass of the sorbent (mg).

Regeneration studies

The preparation process of the synthetic adsorbents generally involves multi-step procedures that are both time and energy-intensive [37]. Except from that this process often requiring expensive and scarcely available reagents. For this reason, in the research of novel sorbents investigation of regeneration potential of them has great importance. In the literature, there are approaches exist for adsorbent regeneration, including biological techniques employing microorganisms, thermal methods via oxidative treatment, and chemical regeneration in which the retained adsorbate is released by treatment with suitable solvents [38]. In the present work, we used chemical regeneration method by investigating the influence of different acids.

Desorption experiments were performed using 0.5 mol·L^{-1} aqueous solutions of HNO_3, HCl, H_2SO_4, H_3PO_4 and CH_3COOH. The first step of experiment is the preparation of sorbents. For this 30 mg of the sorbent was weighted and added to each 5 experiment bottles then 2 ml 10^{-2} M metal solution then 18 mL of a pH 3 buffer solution was added onto them. The suspensions were maintained for 24 h to reach equilibrium then the solid phase was separated from the liquid by filtration.

In the next step, for the controlling desorption potential of each acids, 20 mL of 0.5 mol·L^{-1} solutions of acids were added onto dry sorbent samples and kept for 24 hours. After it, each sample measured and desorption capacity calculated.

ISNN: print 2663-7006; online 2709-2666

RESULTS AND DISCUSSION

Effect of pH on the sorption of Cd (II)

The pH of the solution is one of the most critical factors affecting the sorption of Cd (II) ions, since it controls both the ionization state of functional groups on the sorbent surface and the stability of cadmium in aqueous systems. At low pH values (pH < 4), the high concentration of H^+ ions compete strongly with Cd^{2+} for the active sorption sites, resulting in reduced uptake. In the range of pH 4–8, Cd^{2+} remains the predominant soluble species and electrostatic repulsion is minimized, thereby favoring sorption. However, at higher pH values (pH > 8), cadmium undergoes hydrolysis, leading to the formation of $Cd(OH)^+$, $Cd(OH)_2^-$, and $Cd(OH)_3^-$, $Cd(OH)_4$,$Cd_4(OH)_4$ which can precipitate from solution [39]. To avoid precipitation effects and ensure that the removal process is attributable solely to surface sorption, the initial solution pH was adjusted between 2.0 and 8.0.

The experiment was carried out by weighing and collecting 30 mg of sorbent in different reagent bottles, adding 2 ml of 10^{-2} M metal ion solution and 18 ml of the proper pH, and then letting it remain for 24 hours.

The effect of the pH of the solution on the sorption of cadmium in static and dynamic condition is shown in the figure below (fig 1). As a result of the measurement, it was found that the capture of Cd (II) ions with the highest percentage from the solution was at pH 3 in all three conditions but with different sorption capacity. Therefore, this value of pH was used in all subsequent experiments.

Effect of time on the sorption of metal ions

To investigate the time-dependent nature of sorption, 30 mg of sorbent was mixed with 2 ml of 10^{-2} M metal solution, followed by 18 ml of pH 3. The rate of metal ion sorption in the solution was then monitored for 30 to 270 minutes. It was found that the sorption has already became stable and attained the equilibrium condition after 60 minutes, as shown in figure 2.

One may say that the metal ion was no longer drawn out of the solution after this point. When 1-[1-Methyl-2-(methylamino)ethyl] thiourea was absorbed into the sorbent, the same thing happened but with higher sorption capacity. In other words, the sorption hit the plateau after 60 minutes in both static/dynamic condition for pure sorbent and after modification. The picture below provides a graphical depiction of the experiment's result (fig.2).

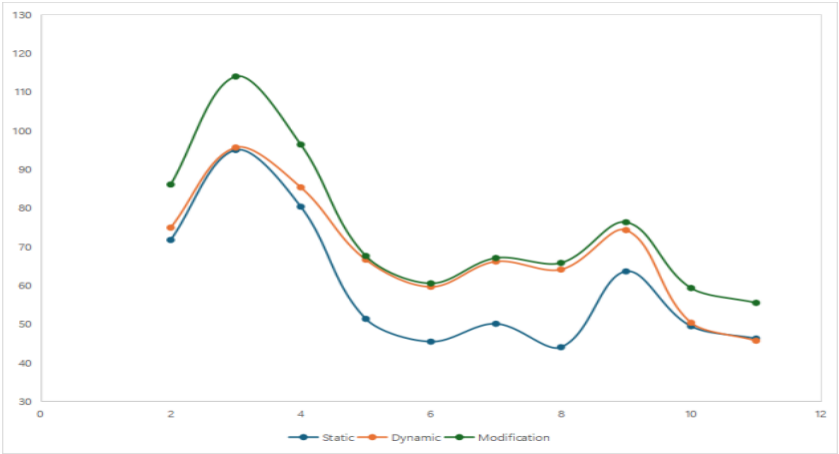

Fig.1. Effect of pH on the sorption of cadmium

Effect of initial concentration of Cd (II) ions on adsorption capacity.

The impact of concentration on the degree of adsorption by the synthesized sorbent was investigated throughout the experiment. Cd (II) ion concentrations ranging from 2 $x10^{-4}$ mol/L to 8 $x10^{-3}$ mol/L were employed for this purpose. This was accomplished by weighing 30 mg of sorbent and adding the proper amount of metal ion solution and pH 3.0. The experiment's outcome is showen in figure 3 below.

Desorption process.

The study of the opposing process, desorption, is also included in the present work. Having the eluents needed to desorb the metal ion is a crucial task. So, by employing several inorganic acids of the same concentration as 0.5 mol/L solutions of HNO_3, HCl, H_2SO_4, CH_3COOH and H_3PO_4 to carry out this procedure. According to the study's findings, 0.5 mol/L H_3PO_4 solution has the highest desorption capability for Cd (II) ions.

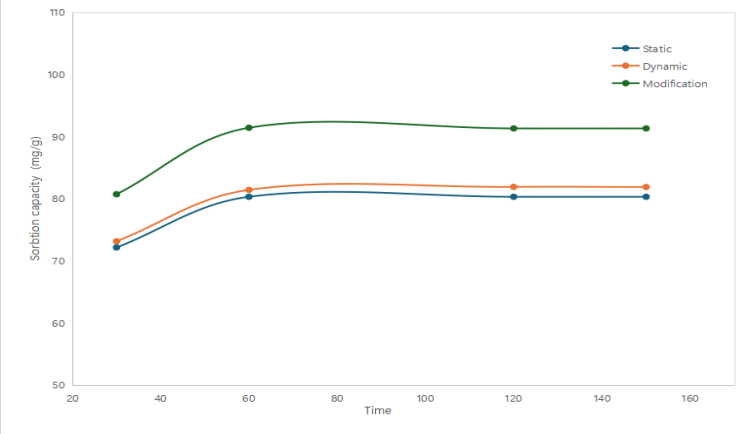

Fig.2. Effect of time to sorption process

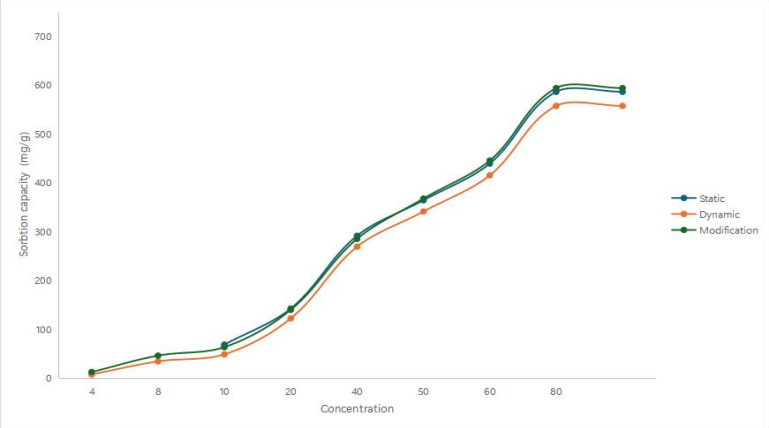

Fig.3. Effect of initial concentration on adsorption capacity

Adsorption isotherm

In these types of studies, it is necessary to have a deeper comprehension of the adsorption process. For that aim, utilizing the appropriate adsorption equilibrium reaches our help. Adsorption equilibrium describes the nature of the interaction between

ISNN: print 2663-7006; online 2709-2666

the adsorbent and the adsorbate. The Langmuir, Freundlich, Dubinin-Radushkevich, Temkin, Redlich–Peterson isotherms were used to examine the equilibrium data in this study.

Langmuir Isotherm

The Langmuir isotherm is one of the most widely applied models for describing adsorption equilibrium. It is based on the fundamental assumption that the surface of the adsorbent is homogeneous, meaning all adsorption sites are energetically equivalent. According to this model, adsorption takes place at specific sites on the surface in a monolayer fashion, with no lateral interactions between adjacent adsorbed molecules. Furthermore, the probability of adsorption at a given site is independent of the occupancy of neighboring sites [40].

The mathematical representation of the Langmuir isotherm is given as:

$$q_e=\frac{q_m K_L C_e}{1+K_L C_e}$$

where C_e (mmol/L) is the equilibrium concentration of the adsorbate in the solution, q_e (mmol/g) is the equilibrium adsorption capacity, q_m represents the maximum adsorption capacity corresponding to complete monolayer coverage, and K_L is the Langmuir constant related to the affinity of the binding sites (L/mmol).

Experimentally, the model can be linearized by plotting 1/ q_e against 1/ C_e. From the slope and intercept of the resulting straight line, the values of q_m and K_L can be determined, respectively.

An additional parameter used to characterize the Langmuir isotherm is the dimensionless equilibrium factor, R_L expressed as:

$$R_L= \frac{1}{1+bC_0}$$

where b is the Langmuir constant (L/mmol) and C_0 is the initial concentration of the adsorbate (mmol/L). The value of R_L provides insight into the favorability of the adsorption process. Specifically, $0 < R_L < 1$ indicates favorable adsorption, while values outside this range signify unfavorable, linear, or irreversible adsorption.

Calculations show the correlation coefficients (R^2) are 0.0282, 0.6619 and 0.4996, respectively for static, dynamic and modification cases. The results indicate that the separation factor (R_L) ranges from 0 to 1 is favorable but in our case the values are minus for all cases. So, it shows that this model doesn't fit (fig. 4).

Freundlich Isotherm

The Freundlich isotherm is an empirical model that describes adsorption on heterogeneous surfaces with non-uniform distribution of adsorption heat and affinities. Unlike the Langmuir model, which assumes surface homogeneity, the Freundlich model accounts for the presence of multiple adsorption sites of varying energies [41].

The isotherm is expressed by the logarithmic form:

$$\ln q_e = \ln K_F + \frac{1}{n} \ln C_e$$

where q_e (mmol/g) represents the adsorption capacity at equilibrium, C_e (mmol/L) is the equilibrium adsorbate concentration, K_F is the Freundlich adsorption

constant indicative of adsorption capacity, and 1/n is the heterogeneity factor that reflects the adsorption intensity.

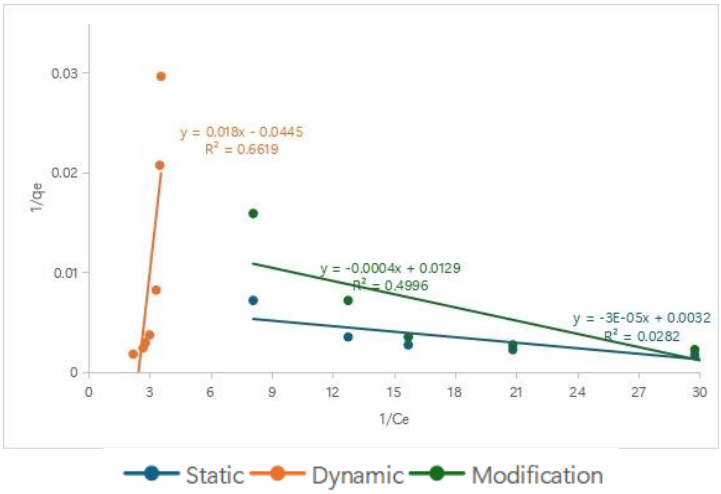

Fig. 4. Langmuir isotherm model

The parameter n provides important insight into the favorability of adsorption. Values of $1 < n < 10$ generally indicate favorable adsorption conditions. A higher n value (corresponding to a smaller 1/n) suggests stronger binding interactions between the adsorbent and adsorbate, while 1/n =1 corresponds to linear adsorption, which implies uniform adsorption energies across the surface. Linear adsorption is typically associated with low solute concentrations and minimal adsorbent coverage. In our the values of 1/n is -1.545, 5.782, 2.790 for static, dynamic and modification cases, respectively (fig.5).

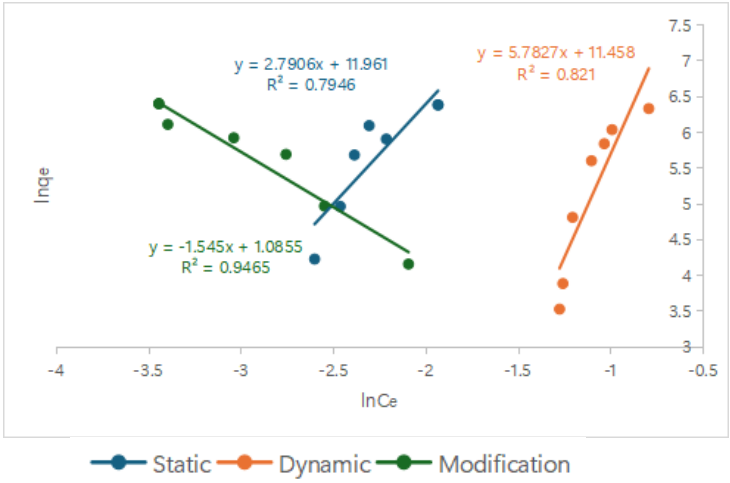

Fig. 5.Freundlich isotherm model

Dubinin–Radushkevich (D–R) Isotherm

The Dubinin–Radushkevich (D–R) isotherm model is frequently employed to evaluate adsorption properties such as porosity, sorption energy, and the mechanism of interaction. Unlike the Langmuir model, it does not assume a uniform surface or

ISNN: print 2663-7006; online 2709-2666

constant adsorption potential, making it more suitable for describing adsorption on heterogeneous surfaces [42]. The general form of the D–R isotherm is expressed as:

$$\ln_e = \ln q_s - k_{D\text{-}R}\varepsilon^2$$

where q_e (mmol/g) is the equilibrium adsorption capacity, q_s represents the theoretical maximum adsorption capacity (mmol/g), $k_{D\text{-}R}$ is the D–R constant related to adsorption energy, and ε is the Polanyi potential.

The Polanyi potential is defined as:

$$\varepsilon = RT \ln\left(1+\frac{1}{C_e}\right)$$

where R is the universal gas constant (kJ·mol^{-1}·K^{-1}), T is the absolute temperature (K), and C_e is the equilibrium concentration of the adsorbate (mmol/L).

A significant feature of the D–R isotherm is its ability to distinguish between physical and chemical adsorption processes. The mean free energy of adsorption (E) can be calculated from the constant $k_{D\text{-}R}$ obtained from the slope of the plot, according to:

$$E = \frac{1}{\sqrt{2k_{D\text{-}R}}}$$

where E (kJ/mol) indicates the type of sorption mechanism. Typically, values of E < 8 kJ/mol suggest physical adsorption driven by weak Van der Waals forces, whereas values of E > 8 kJ/mol are indicative of chemisorption involving charge transfer or chemical bonding.

The obtained R^2 values are 0.8275, 0.8634,0.917 and the calculated adsorption energy (E) is 1 and 5 kJ/mol for static and dynamic studies. According to the established criteria, an E value in the range of 8–16 kJ/mol suggests chemisorption, whereas values below 8 kJ/mol are indicative of physisorption. Therefore, in both cases, the E value being less than 8 kJ/mol suggests that the adsorption process is predominantly physical in nature (fig.6).

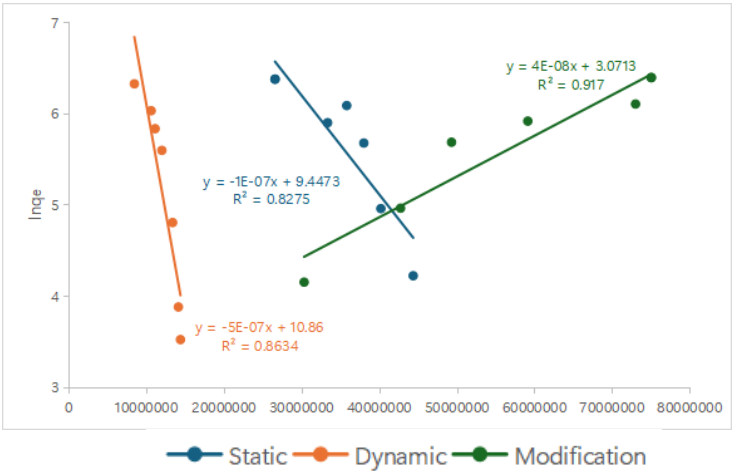

Fig. 6. Dubinin-Radushkevich (D-R) isotherm

Temkin Isotherm

The Temkin isotherm model considers the effects of indirect adsorbate–adsorbate interactions on the adsorption process. Unlike the Langmuir model, which assumes

constant adsorption energy, the Temkin model proposes that the heat of adsorption decreases linearly with increasing surface coverage due to these interactions [43]. This assumption provides a more realistic description of adsorption behavior, particularly at intermediate concentrations.

The Temkin equation is expressed in both its general (I) and linearized forms (II):

$$q_e=\frac{RT}{b_T}\ln(K_T C_e) \quad (I)$$

$$q_e=\frac{RT}{b_T}\ln(K_T)+\frac{RT}{b_T}\ln(C_e) \quad (II)$$

where q_e (mmol/g) is the adsorption capacity at equilibrium, C_e (mmol/L) is the equilibrium adsorbate concentration, K_T (L/g) is the Temkin isotherm constant, R (8.314 J·mol^{-1}·K^{-1}) is the universal gas constant, T (K) is the absolute temperature, and b_T (J/mol) is a constant related to the heat of adsorption.

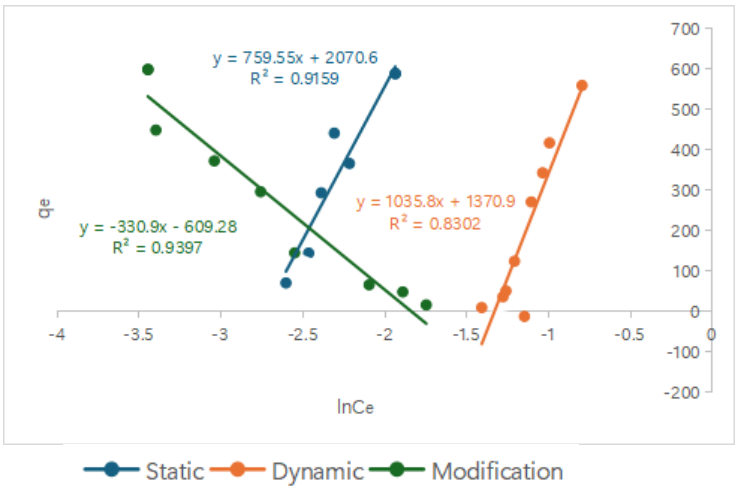

Fig.7. Temkin isotherm model

As shown in figure 7, static condition B_T value is 759.55 kJ/mol ; following in the dynamic case , this value rises to 1035.8 kJ/mol. Since B_T values below 8 kJ/mol are generally linked to physisorption, this suggests that the adsorption process is primarily physical before functionalization. In both cases, B_T value marginally surpasses 8 kJ/mol that indicating chemisorption. In terms of the K_T value, it changes from 15.27 to 3.757 in static and dynamic absorption conditions and 6.305 after modification.From this values we can say that in the static condition adsorbant surface has highest affinity.

Redlich–Peterson Isotherm

The Redlich–Peterson (R–P) isotherm is a hybrid model that incorporates features of both the Langmuir and Freundlich isotherms. It is widely applied because of its ability to describe adsorption over a broad concentration range, including both homogeneous and heterogeneous surface conditions [44]. Unlike strictly empirical models, the R–P isotherm provides a semi-empirical framework that bridges the assumptions of ideal monolayer adsorption and multilayer adsorption on heterogeneous sites.

ISNN: print 2663-7006; online 2709-2666

The non-linear form of the R–P equation is expressed as:

$$q_e = \frac{K_R C_e}{1+a_R C_e^{\beta}}$$

where q_e (mmol/g) is the adsorption capacity at equilibrium, C_e (mmol/L) is the equilibrium concentration of the adsorbate, K_R (L/g) is the R–P constant related to adsorption capacity, a_R (L/mmol) is a constant, and β is an exponent with a value between 0 and 1.

The parameter β plays a crucial role in determining the model's behavior. When $\beta = 1$, the R–P equation reduces to the Langmuir form, suggesting adsorption on a homogeneous surface. Conversely, when $\beta < 1$, the equation resembles the Freundlich model, indicating adsorption on heterogeneous surfaces.

Due to this flexibility, the R–P isotherm is particularly valuable for systems where neither the Langmuir nor the Freundlich models alone adequately describe adsorption, thus making it a powerful tool for interpreting experimental sorption data.

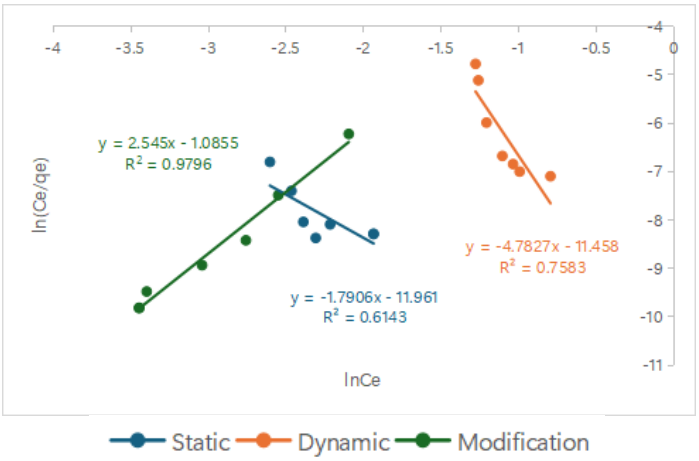

Fig.8. Redlich–Peterson Isotherm

These results show that (fig.8) the three systems differ from one another. Stronger interactions under altered conditions were observed by the modified cases with larger a/K ratio and greater slope g = 2.545. On the other hand, both the dynamic and static systems showed negative values of g, which are beyond the range of $0 < g < 1$ that theoretically acceptable.

CONCLUSION

To sum up, our research yielded encouraging and significant findings that demonstrate the effectiveness of this innovative functionalized sorbent in removing cadmium from water. Adsorption capacity rises by around 20% after sorbent's modification with novel thiourea derivative in static coundition and almost same results were observed in dynamic condition. Several isoterm models were used to study adsorption process and the Redlich–Peterson Isotherm model was determined to provide the greatest match. From the Temkin isoterm, it was calculated that there is chemisorption.

REFERENCES

1. Pradinaud C., Northey.S., Amor.B., et al .Defining freshwater as a natural resource: A framework linking water use to the area of protection natural resources. Int J Life Cycle Assess. 2019, pp. 960-974. doi: 10.1007/s11367-018-1543-8
2. Tchounwou P.B., Yedjou C.G., Patlolla A.K., Sutton D.J.Exp Suppl. Heavy metal toxicity and the environment.Exp Suppl. 2012, pp.133-64. doi: 10.1007/978-3-7643-8340-4_6
3. Khan Z., Elahi A., Bukhari D. A., Rehman A. Cadmium sources, toxicity, resistance and removal by microorganisms-A potential strategy for cadmium eradication. Journal of Saudi Chemical Society. 2022, Vol.26, Issue 6, pp. 1-18 doi.org/10.1016/j.jscs.2022.101569
4. Rahimzadeh R., Rahimzadeh R., Kazemi S., Moghadamnia A.Cadmium toxicity and treatment: An update.Caspian J.Intern Med. 2017, pp. 135-145. doi: 10.22088/cjim.8.3.135
5. Briffa J., Sinagra E., Blundell R. Heavy metal pollution in the environment and their toxicological effects on humans. Heliyon. 2020. Vol.6, Issue 9,pp. 1-26. https://doi.org/10.1016/j.heliyon.2020.e04691
6. Uddin S., Khanom S., Islam M.R., Hossain, M. Cadmium Contamination: Sources, Behavior, and Environmental Implications. In: Kumar, N. (eds) Cadmium Toxicity. Springer, Cham. 2024, pp. 67-101. https://doi.org/10.1007/978-3-031-65611-8_4
7. Qu F, Zheng W. Cadmium Exposure: Mechanisms and Pathways of Toxicity and Implications for Human Health. Toxics. 2024, pp. 1-15. doi: 10.3390/toxics12060388
8. Yang Y, Hassan M.F., Ali W., Zou H., Liu Z., Ma Y. Effects of Cadmium Pollution on Human Health: A Narrative Review. Atmosphere. 2025, pp. 1-23. doi: 10.3390/atmos16020225
9. Chunhabundit R. Cadmium Exposure and Potential Health Risk from Foods in Contaminated Area, Thailand. Toxicol Res. 2016, pp.65-72. doi: 10.5487/TR.2016.32.1.065
10. Yan L.J., Allen D.C. Cadmium-Induced Kidney Injury: Oxidative Damage as a Unifying Mechanism. Biomolecules. 2021,pp.1-17. doi: 10.3390/biom11111575
11. Hong D., Min J.Y., Min K.B. Association Between Cadmium Exposure and Liver Function in Adults in the United States: A Cross-sectional Study. J Prev Med Public Health. 2021, pp.471-480. doi: 10.3961/jpmph.21.435
12. Akesson A., Bjellerup P., Lundh T., Lidfeldt J., Nerbrand C., Samsioe G., Skerfving S., Vahter M. Cadmium-induced effects on bone in a population-based study of women. Environ Health Perspect. 2006, pp. 830-834. doi: 10.1289/ehp.8763
13. Akesson. A, Bjellerup. P , Lundh.T, Lidfeldt . J., Nerbrand. C, Samsio.G, Skerfving.S, Vahter M. Cadmium-induced effects on bone in a population-based study of women. Environ Health Perspect. 2006, pp. 830-834. doi: 10.1289/ehp.8763
14. Rikans.L.E, Yamano.T. Mechanisms of cadmium-mediated acute hepatotoxicity. J. Biochem Mol Toxicol. 2000, pp. 110-117. doi: 10.1002/(sici)1099-0461(2000)14:2<110::aid-jbt7>3.0.co;2-j
15. Bautista.C.J ; Arango. N ; Plata .C ; Mitre Aguilar I.B ; Trujillo . J ; Ramírez .V. Mechanism of cadmium-induced nephrotoxicity. Toxicology. 2024, pp. 1-13. doi:

ISNN: print 2663-7006; online 2709-2666

10.1016/j.tox.2024.153726
16. Kumar.S , Sharma.A. Cadmium toxicity: Effects on human reproduction and fertility. Rev Environ Health. 2019, pp. 327-338. doi: 10.1515/reveh-2019-0016
17. Tellez-Plaza . M , Jones . M.R , Dominguez-Lucas . A , Guallar. E , Navas-Acien. A. Cadmium exposure and clinical cardiovascular disease: A systematic review. Curr Atheroscler Rep. 2013, pp.1-15. doi: 10.1007/s11883-013-0356-2
18. Knoell. D.L , Wyatt . T.A. The adverse impact of cadmium on immune function and lung host defense. Semin Cell Dev Biol. 2021, pp. 70-76. doi: 10.1016/j.semcdb.2020.10.007
19. Hartwig. A. Cadmium and cancer. Met Ions Life Sci. 2013, pp. 491-507. doi: 10.1007/978-94-007-5179-8_15
20. Kazantzis. G. Cadmium, osteoporosis and calcium metabolism. Biometals. 2004, pp. 493-498. doi: 10.1023/b:biom.0000045727.76054.f3
21. Bonaventura. P , Courbon. G , Lamboux. A. Protective effect of low dose intra-articular cadmium on inflammation and joint destruction in arthritis. Sci Rep. 2017, pp.1-11. doi: 10.1038/s41598-017-02611-5
22. Hu. X, Kim. K.H , Lee . Y, Fernandes . J , Smith . M.R , Jung. Y.J , Orr. M, Kang . S.M , Jones.D.P., Go.Y.M. Environmental Cadmium Enhances Lung Injury by Respiratory Syncytial Virus Infection. Am J Pathol. 2019, pp.1513-1525. doi: 10.1016/j.ajpath.2019.04.013
23. Horiguchi.H.; Oguma. E; Kayama. F. Cadmium induces anemia through interdependent progress of hemolysis, body iron accumulation, and insufficient erythropoietin production in rats. Toxicol Sci. 2011, pp.198-210. doi: 10.1093/toxsci/kfr100
24. Verzelloni. P; Giuliano. V; Wise. L.A; Urbano. T, Baraldi. C., Vinceti. M., Filippini.T. Cadmium exposure and risk of hypertension: A systematic review and dose-response meta-analysis. Environ Res. 2024, pp. 1-10. doi: 10.1016/j.envres.2024.120014
25. Nehzomi .Z.S, Shirani. K. The gut microbiota: A key player in cadmium toxicity – implications for disease, interventions, and combined toxicant exposures. J Trace Elem Med Biol. 2025, pp. 1-10. doi: 10.1016/j.jtemb.2024.127570
26. Mititelu. M, Neacșu. S.M, Busnatu .Ș.S, Scafa-Udriște .A, Andronic .O, Lăcraru A-E, Ioniță-Mîndrican C.-B., Lupuliasa D., Negrei C., Olteanu G. Assessing contamination in Food: Implications for Human Health and Environmental Safety. Toxics. 2025, pp.1-49. doi: 10.3390/toxics13050333
27. Farias. J.P; Okeke. B.C; Demarco. C.F; Carlos. F.S ; da Silva.R.F; da Silva.M.A ; Quadro M.S.; Pieniz S.; Andreazza R. Cadmium Contamination in Aquatic Environments: Detoxification Mechanisms and Phytoremediation Approach. Sustainability. 2024, pp.1-24. doi: 10.3390/su162210072
28. Yusuf. B.O, Aliyu. M., Azeez .M.O., Taialla. O.A., Lateef. S., Sulaimon. R., Akinpelu. A.A, Ganiyu.S.A. Comprehensive technologies for heavy metal remediation: Adsorption, membrane processes, photocatalysis, and AI-driven design. Desalination. 2025, pp.1-8. doi: 10.1016/j.desal.2025.119261
29. Satyam. S, Patra. S. Innovations and challenges in adsorption-based wastewater remediation: A comprehensive review. Heliyon. 2024, pp.1-24. doi: 10.1016/j.heliyon.2024.e29573
30. Dehghani M.H., Ahmadi S., Ghosh S., et.al. Recent advances on sustainable adsorbents for the remediation of noxious pollutants from water and wastewater: A

critical review. Arabian Journal of Chemistry. 2023, pp.1-29. https://doi.org/10.1016/j.arabjc.2023.105303
31. Rashid A.B., Haque M., Islam S. Nanotechnology-enhanced fiber-reinforced polymer composites: Recent advancements on processing techniques and applications. Heliyon. 2024, pp.1-29. https://doi.org/10.1016/j.heliyon.2024.e24692
32. Raja S., Mattoso L.H.C. Functionalized Polymer-Based Composite Photocatalysts. Green Photocatalysts. Springer. 2020, pp.167-188. https://doi.org/10.1007/978-3-030-15608-4_7
33. Hernández-Cruz O., Córdova-Pérez G.E., Cortez J.R.C. Functional polymeric materials for hard water treatment a comprehensive review.Discov Mater.2025, pp. 1-40. https://doi.org/10.1007/s43939-025-00360-1
34. Sucayev Ə.R. Aminspirtlər əsasında bəzi tiokarbamid törəmələrinin sintezi və tədqiqi. Journal of Qafqaz University- Chemistry and Biology.2016, pp. 92-100.
35. Javadzade T., Rzayeva I., Demukhamedova S., Akverdieva G., Farzaliyev V., Sujayeva A.,Chiragov F. Synthesis, structural analysis, DFT study, antioxidant activity of metal complexes of N-substituted thiourea. Polyhedron. 2023. pp 1-16. https://doi.org/10.1016/j.poly.2022.116274
36. Otomo M. The Spectrophotometric Determination of Cadmium with Xylenol Orange. Bulletin of the Chemical Society of Japan. 1964, pp.504-508. https://doi.org/10.1246/bcsj.37.504
37. Akhtar M.S., Ali S., Zaman W. Innovative Adsorbents for Pollutant Removal: Exploring the Latest Research and Applications. Molecules. 2024, pp.1-37. https://doi.org/10.3390/molecules29184317
38. Lata S., Singh P.K., Samadder S.R. Regeneration of adsorbents and recovery of heavy metals: a review. Int. J. Environ. Sci. Technol. 2015, pp.1461–1478. https://doi.org/10.1007/s13762-014-0714-9
39. Anielak A.M.,Schmidt R. Sorption of Lead and Cadmium Cations on Natural and Manganese-Modified Zeolite. Polish Journal of Environmental Studies.2011, pp.15-19
40. Kushwaha A.K., Gupta N., Chattopadhyaya M.C. Dynamics of adsorption of Ni (II), Co(II) and Cu(II) from aqueous solution onto newly synthesized poly[N-(4-[4-(aminophenyl)methylphenylmethacrylamide])]. Arabian Journal of Chemistry. 2017, pp.1-9. https://doi.org/10.1016/j.arabjc.2013.06.007
41. Anah L., Astrini N. Isotherm adsorption studies of Ni (II) ion removal from aqueous solutions by modified carboxymethyl cellulose hydrogel. IOP Conf. Series: Earth and Environmental Science. 2018, pp.1-9. https://doi.org/10.1088/1755-1315/160/1/012017
42. Hu Q., Zhang Z. Application of Dubinin–Radushkevich isotherm model at the solid/solution interface: A theoretical analysis. Journal of Molecular Liquids. 2019, pp. 646 - 648. https://doi.org/10.1016/j.molliq.2019.01.005
43. Aharoni C., Ungarish M.Kinetics of activated chemisorptions. Part 2. Theoretical models. J. Chem. Soc. Faraday Trans. 1977, pp. 456–464. https://doi.org/10.1039/F19777300456
44. Redlich, O., Peterson, D.L.: A useful adsorption isotherm. J. Phys. Chem. 1959, pp. 1024-1024

ISNN: print 2663-7006; online 2709-2666

ASOIU
Azerbaijan State Oil and Industry

AJCN, Vol .7, No.1, 2025, pp.18-25
https://doi.org/10.32010/AJCN04022025-18

THE SYNTHESIS OF NEW POLYMER COMPOSITES BASED ON OIL PORPHYRINS

[1] *Minira Aghahuseynova*[0000-0003-2471-2136]
Department of "Chemistry and technology of inorganic substances"
Professor, doctor of chemical sciences,
Azerbaijan State Oil and Industrial University
minira_baku@yahoo.com
[2]*Maleyka Azizova*[0009-0007-2066-8074]
Department of "Chemistry and technology of inorganic substances"
Master, Azerbaijan State Oil and Industrial University
azizovameleyke04@gmail.com

Abstract: *This research on the synthesis of composite materials based on heavy oil residues possesses scientific novelty in several aspects. In the contemporary stage of industrial development, the increasing waste load of the oil refining industry, along with the growing demand for high-performance and durable materials, necessitates new approaches for scientific and technological advancement. For the first time, polymer composites have been developed based on petroleum porphyrins isolated from asphaltene–resin–paraffin residues. A new synthesis method for polymer composite materials based on petroleum porphyrins isolated from the asphaltene–resin–paraffin residues of the Buzovna field has been proposed. This approach contributes to solving the environmental problem associated with the utilization of heavy oil residues. The observed spectroscopic changes can be explained by the fact that the immobilization of the porphyrin occurs through the formation of ionic bonds between the functional groups of the porphyrin and the positively charged nitrogen atoms of chitosan, resulting in the formation of an insoluble polyelectrolyte complex. Thus, the results indicate that only chitosan effectively binds to the porphyrin, whereas methylcellulose remains inert.*
Keywords: *composite material, oil residues, chitosan, methylcellulose, biocompatible polymer.*

INTRODUCTION

The effectiveness of drugs can be enhanced through their immobilization in polymer carriers. The use of polymers enables the imparting of important properties to already known drugs, such as increased stability, controlled solubility, and reduced toxicity. In the future, applied studies on the physiological activity of polymers should lead to the development and introduction into practical medicine of a new generation of pharmaceuticals characterized by prolonged action, controlled pharmacokinetics, and targeted delivery to specific organs.

An important application area of porphyrins and their analogues is medicine. Based on their preferential accumulation in tumor cells and their photoluminescent ability to generate cytotoxic oxygen, research on porphyrins as sensitizers for the photodynamic therapy of oncological diseases is developing intensively.

However, despite their many positive qualities, porphyrins exhibit only short-term therapeutic effects, which necessitates frequent administration. To achieve prolonged drug action, viscosity regulators are employed, and the use of a new polymer form in the shape of a film, based on biologically active substances containing pharmaceuticals derived from petrochemical synthesis, has been proposed.

In ophthalmology, the most commonly used dosage forms are eye drops (solutions, suspensions), ointments and gels, as well as ocular films. The search for new

drug forms that allow reduced administration without diminishing therapeutic efficacy is of great scientific and practical interest. The use of long-acting drug formulations decreases the likelihood of overdose and mitigates the adverse effects of frequent instillations, while also relieving patients and medical staff from repeated manipulations. In this regard, the development and application of ocular drug films would represent a rational solution to the problem of achieving prolonged therapeutic effects and ensuring the targeted delivery of effective antibiotics to ocular tissues.

The use of drugs in the form of ocular films reduces both ocular toxicity and systemic side effects, since the drug is gradually released from the films and delivered to the conjunctiva and cornea in a prolonged and uniform manner, while minimizing the amount lost through lacrimal drainage into the nasal cavity. The valuable properties of ocular drug films also include their stability, allowing storage for up to two years, high sterility, reduced risk of infection, ease of placement on the conjunctival membrane, and lower drug consumption due to less frequent administration compared to eye drops. Furthermore, immobilization of drugs within films eliminates disadvantages such as the unpleasant taste of bitter or nauseating medicines, ensures their targeted delivery to the desired area of the body, and provides the basis for the development of various diagnostic products. A wide range of synthetic and natural polymers is widely used as materials for the production of such films.

Porphyrins are included in the composition of many drugs; however, as is well known, all drugs have a limited duration of action after which they are eliminated from the body. Moreover, the smaller the molecular weight of the drug, the faster it is excreted. For prolonged pharmacological effects, it has been proposed to graft physiologically active compounds with hydrolyzable ester bonds, salts, and other functional groups onto carrier polymers.

One of the rapidly developing areas in recent years is the fixation of active metalloporphyrins into polymer matrices. A review of the literature shows that the mode of attachment of porphyrins to polymer matrices is diverse. In several studies, the immobilization of porphyrins and their complexes was achieved through coordination bonds. The interaction of porphyrins with polymers occurs via the formation of secondary amines, esters, and other functional groups as a result of the interaction between the functional groups of polymers and porphyrins. In these works, the immobilization of porphyrins and metal complexes was confirmed using electronic and IR spectroscopy, elemental analysis for nitrogen, as well as spectrophotometric methods to determine the mass fractions of metals in polymer metalloporphyrins.

The analysis of the literature indicates that polymer-bound porphyrins are significant in terms of their therapeutic effects. Nevertheless, research on the synthesis of porphyrins and their metal derivatives remains limited. Therefore, the development of new methods for immobilizing porphyrins and their metal derivatives in polymer matrices, along with expanding their application fields, is undoubtedly of great interest.

Furthermore, the potential modification of metalloporphyrins derived from heavy petroleum residues may stimulate the advancement of more efficient and cost-effective technologies for the production of effective pharmaceuticals.

EXPERIMENTAL PART

The research object was the ASPO collected from the Buzovna field of “Tagiyev Operating Company” Intertek Azeri LTD. The content of asphaltenes, resins, and

ISNN: print 2663-7006; online 2709-2666

paraffins in the field samples was determined according to GOST 11851-85 "Oil. Method for the determination of paraffin."

X-ray fluorescence analysis of solid deposits was carried out using an X-ray fluorescence spectrometer to determine the presence and quantitative composition of metals in ASPO. Sample measurements were conducted in the range of 0.0–16.0 keV.

IR spectroscopy analysis was performed at 20 °C using a NICOLET 5700 FT-IR Fourier transform infrared spectrometer in the range of 400–4000 cm^{-1}. Paraffin, asphaltene, resin, and composite samples were pressed into KBr pellets. The baseline correction was conducted using the OPUS software.

UV spectrometry analysis of free porphyrins, collected in 10 ml fractions at the outlet of the cylinder, was performed on an Evolution 300 UV/VIS spectrophotometer (USA) using quartz cuvettes with a thickness of 10 mm at 700 nm. The spectral type of porphyrins was determined by the ratio of the intensities of the I, II, III, and IV absorption bands.

The UV spectra of aqueous solutions of drugs were also recorded on an Evolution 300 UV/VIS spectrophotometer (USA) using 10 mm quartz cuvettes. The drug concentrations were determined using calibration curves based on the absorption maxima characteristic of each drug.

For the preparation of a chitosan/methylcellulose composite material based on petroleum porphyrins, chitosan and methylcellulose were used as raw materials, and the process was carried out using the methods described below.

Chitosan (Chitosan, Practical Grade from Crab Shells) with a molecular mass of 3.5–250 kDa and a degree of deacetylation of 70 (fig.1.) was produced by Sigma (USA) and used without additional purification.

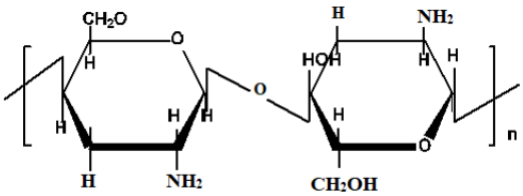

Fig. 1. The chemical structure of chitosan

Methylcellulose (MC) (fig.2.) was produced by Sigma (USA) and used without additional purification.

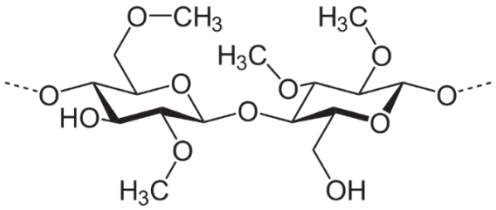

Fig. 2. Chemical structure of methylcellulose

Polyvinyl alcohol (PVA) with a molecular weight of 90 kDa, produced by Sigma (USA), was used without additional purification. It has a degree of hydrolysis of 86.7–88.7 mol% and a residual acetate group content of 10.0–11.6%. PVA dissolves in water when heated up to 60 °C.

A 2% chitosan solution was prepared in 0.1 M acetic acid in a beaker, which was then placed on a magnetic stirrer until the chitosan was completely dissolved.

Separately, a 1% methylcellulose solution was prepared by dissolving it in distilled water. The polymer ratio was set at 75:25. The calculated amount of porphyrin (150 mg/g) was added to the filtered polymer solution under stirring. The resulting polymer solution was poured into Petri dishes and dried at room temperature for 2–3 days. The dried biopolymer samples were carefully removed from the Petri dishes and placed in a 5% NaOH solution to neutralize residual acetic acid, followed by washing with ethanol to remove excess alkali. The modified samples were then rinsed with distilled water and dried in air.

Method for the preparation of polymer composites containing Mitomycin-C:

Upon heating, a 1.5% chitosan solution was prepared by dissolving chitosan in 0.1 M hydrochloric acid. The solution was placed on a magnetic stirrer until the chitosan was completely dissolved. Separately, an 8% PVA solution was prepared in distilled water. The cooled 1.5% chitosan solution was then combined with the PVA solution. The polymer ratio was set at 75:25. The calculated amount of immobilized Mitomycin-C (125 mg/g and 250 mg/g) was added to the filtered polymer solution under stirring. The resulting solution was poured into Petri dishes and left on a horizontal surface at room temperature for 2–3 days. The obtained dry composite samples were carefully removed from the molds, immersed in a 5% NaOH solution to neutralize residual acid, and subsequently washed with ethanol to remove excess NaOH.

To obtain cross-linked films, 2% chitosan was dissolved in an aqueous 1% hydrochloric acid solution upon heating and then stirred on a magnetic stirrer for 4–5 hours. The calculated amount of immobilized Mitomycin-C (125 mg/g) was added to the filtered polymer solution under stirring. For subsequent cross-linking, an aqueous 0.05% glutaraldehyde solution was added to the polymer solution containing Mitomycin-C. The resulting polymer solution was poured into Petri dishes and dried at room temperature for 2–3 days. The dried biopolymer composites were carefully removed from the Petri dishes, immersed in a 5% NaOH solution to neutralize residual acetic acid, and then washed with ethanol to remove excess alkali.

A 1.5% chitosan solution was combined with an 8% polyvinyl alcohol solution. The polymer ratio was set at 75:25. The anticancer drug Mitomycin-C (125 mg/g and 250 mg/g) was then added to the resulting polymer solution.

RESULTS AND DISCUSSION

One of the approaches to enhancing the effectiveness of cancer chemotherapy, particularly in the treatment of malignant neoplasms, is the use of new polymer composite systems in the form of films containing immobilized anticancer drugs. The implantation of such systems at the tumor site allows for the sustained generation of high concentrations of the drug directly in the vicinity of cancer cells.

The current arsenal of oncological agents is limited, and many of these drugs have several drawbacks, including a short duration of antitumor effect and systemic toxicity. One approach to overcoming these limitations is the use of fundamentally new polymer composite systems in the form of films based on petroleum porphyrins. These systems are employed in the treatment of cancers of various organs, including the lungs, eyes, ovaries, mammary glands, stomach, pancreas, and bladder, with their antitumor effects exerted directly on malignant tumor cells. Porphyrins are widely used as photosensitizers in the photodynamic therapy of cancer. These drugs are highly active but are characterized by a short duration of action (3–4 hours) and rapid elimination from the body. Among polysaccharides capable of forming films, chitosan is one of the

ISNN: print 2663-7006; online 2709-2666

most widely used in the pharmaceutical industry.

Chitosan (poly(1-4)-2-amino-2-deoxy-β-D-glucan)) is a natural polymer obtained through the alkaline deacetylation of chitin—a linear aminopolysaccharide composed of N-acetyl-2-amino-2-deoxy-D-glucopyranose—and protein compounds derived from other natural sources.

The mechanical and physical properties of biodegradable chitosan films can potentially be enhanced by the addition of suitable polysaccharides such as methylcellulose. This water-soluble cellulose derivative is widely used in the pharmaceutical, cosmetic, and food industries as a binder, thickener, or film stabilizer. Methylcellulose films are less rigid but more flexible compared to chitosan films, whereas chitosan–methylcellulose composite films exhibit intermediate mechanical strength characteristics.

In this study, a comprehensive physicochemical investigation of polymer compositions based on petroleum porphyrins was conducted. To assess the potential chemical interactions among the functional groups of chitosan, methylcellulose, and porphyrin, the infrared spectra of the samples (fig.3 and fiq.4) were recorded and analyzed.

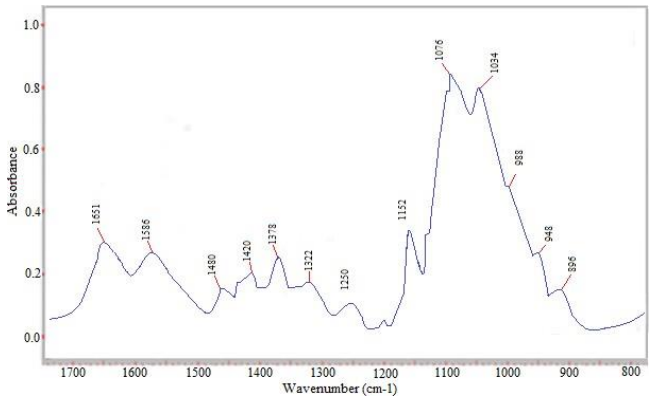

Fig. 3. IR spectra of the chitosan film

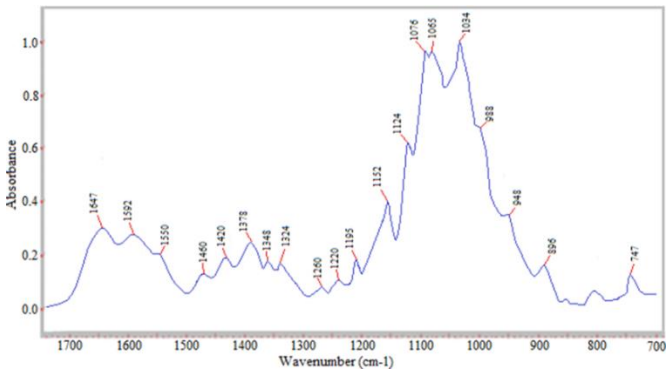

Fig. 4. IR spectra of porphyrin-containing biopolymer film

Bands characteristic of chitosan were observed at 896, 948, 1034, 1076, 1152, 1324, 1378, and 1420 cm^{-1}. In the 1500–1700 cm^{-1} region, some changes occurred due to the binding of porphyrins. Specifically, two chitosan bands at 1586 cm^{-1} (NH_2) and 1651 cm^{-1} (Amide I) shifted to 1592 cm^{-1} and 1647 cm^{-1}, respectively.

The observed spectroscopic changes can be explained by the fact that the immobilization of porphyrin occurs through the formation of ionic bonds between the

functional groups of porphyrin and the positively charged nitrogen atoms of chitosan, resulting in the formation of an insoluble polyelectrolyte complex.

Thus, the results indicate that only chitosan binds effectively to porphyrin, whereas methylcellulose remains inert. The UV–visible (300–700 nm) absorption spectra of porphyrin and porphyrin-containing polymer films are shown in figure 5.

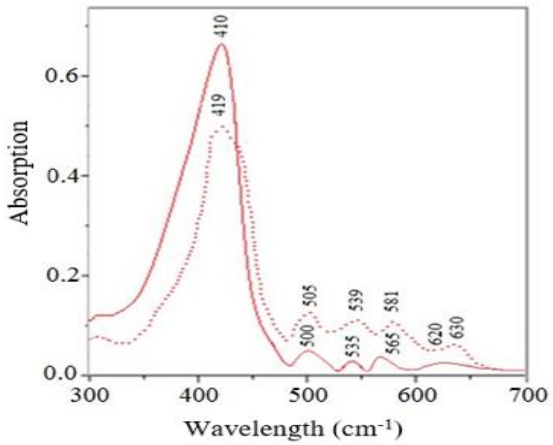

Fig.5. UV absorption spectra: porphyrin (solid), porphyrin-containing polysaccharide film

As seen from the figure, upon interaction with the polymer, the Soret band at 410 nm and the Q-bands of porphyrin (500, 535, 565, and 620 nm) are significantly shifted, indicating the formation of a complex. SEM images of the polymer composite systems are shown in figures 6 a and b.

SEM analysis confirmed that chitosan and chitosan–methylcellulose films possess smooth, uniform surfaces. This is attributed to the porphyrin molecules filling surface voids and smoothing the film surface.

The obtained data demonstrate the feasibility of using chitosan and methylcellulose polysaccharides to develop porphyrin-based film drug formulations. The characterized samples allow for the prediction of drug efficacy and the design of polymer materials that deliver the required amount of porphyrin to the body.

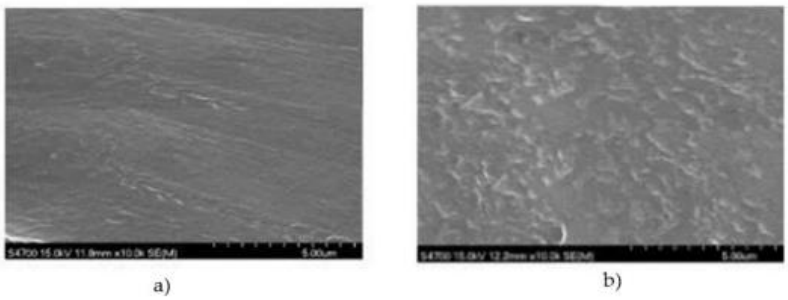

Fig. 6. SEM images of the polymer composites

a) Chitosan containing porphyrins; b) Porphyrin-containing chitosan/methylcellulose

Furthermore, the results of the physicochemical studies indicate that natural polysaccharide chitosan and the water-soluble polymer methylcellulose are highly effective as matrices for the development of new film materials for the treatment of oncological diseases.

ISNN: print 2663-7006; online 2709-2666

CONCLUSION

A method has been developed for obtaining highly efficient extractants for the separation of metalloporphyrin concentrates from heavy petroleum products using highly selective bifunctional organic compounds (ketone alcohols) toward metal porphyrins. The best results were demonstrated by 2-hydroxycyclohexanone. Based on the results of spectral absorption in the visible region, it was established that in all obtained extracts the disappearance of characteristic absorption bands of vanadyl and nickel porphyrins and the appearance of bands characteristic of free porphyrin bases occurred, confirming the demetallization of metalloporphyrins during the extraction process.

The results of physicochemical studies demonstrated the high efficiency of using the natural polysaccharide chitosan and the water-soluble polymer methylcellulose as matrixs for the preparation of new composite materials.

The interaction mechanism of porphyrins with biocompatible polymers has been investigated in connection with the necessity of developing new effective anticancer and therapeutic drugs. Spectroscopic analysis revealed that porphyrin molecules exhibit strong affinity only toward chitosan, while methylcellulose remains inert, showing no interaction.

REFERENCES

1. Achugasim O., Ojinnaka C., Osuji L. Managment of petroporphyrins in a crude oil polluted environment. European Chemical Bulletin. 2013, 2 (10), pp. 794-796 DOI: 10.17628/ecb.2.794-796
2. Aghahuseynova M.M., Abdullaeva G.N. Catalytic of oxygenation of olefins with petroleum metalloporphyrins. Proceedings of Higher Education Institution: Russian Journal of Chemistry and Chemical Technology. 2010, 53 (9), pp 12-16
3. Aghahuseynova M.M., Abdullaeva G.N., Salmanova N.İ. Supramolecular metalloporphyrin catalytic systems for petrochemical synthesis. Oil Refining and Petrochemistry. 2010, pp.172-175
4. Aghahuseynova M.M. Synthesis and properties of metallocomplex catalysts based on oil metalloporphyrins. EURECA -Physics and Engineering. 2020, № 4, pp.19-28.
5. Akhmetov A.F., Krasilnikov Yu.V., Organyuk O.V., Parfenov M.A., Lyapina N.K. On the issue of studying metalloporphyrins in oils. Oil and Gas Business (e-journal). 2012, № 5, pp. 336-342
6. Barona-Castano J., Carmona-Vargas C., Brocksom T., de Oliveira K. Porphyrins as catalysis in scalable organic reactions. Molecules. 2016, 21 (3), 310 p. https://doi.org/10.3390/molecules21030310
7. Berger J., Reist M., Mayer J.M., Felt O., Gurny R. Structure and interactions in chitosan hydrogels formed by complexation or aggregation for biomedical applications. European Journal of Pharmaceutics and Biopharmaceutics. 2004, 57, pp. 35-52
8. Fateeva A., Chater P.A., Ireland C.P., Tahir A.A., Khimyak Y.Z., Wiper P.V., Darwent J.R., Rosseinsky M.J. A water-stable porphyrin-based metal-organic framework active for visible-light photocatalysis. Angewandte Chemie International Edition. 2011, 50 (36), pp. 7496-7500
9. Hugo S.S., Ana C.R., Sodero J-P., Korb J.-P. The role of metalloporphyrins on the

physical-chemical properties of petroleum fluids. Fuel. 2017, 188, pp. 374-381
10. I.B.Beletskaya, Tyurin V.S., Tsivadze A.Y., Guilard R., Stern C. Supramolecular chemistry of metalloporphyrins. Chemical Reviews. 2009, 109 (5), pp.1659-1713
11. İmran M., Qureshi A.K., Tarig M. Emerging applications of porphyrin and metalloporphyrins in biomedicine and diagnostic magnetic resonance imaging. 4Biosensors. 2018, pp. 95-112
12. Magomedov R.N., Popova A.Z., Maryutina T.A., Kadiev Kh.M., Khadziev S.N. State and prospects of demetallization of heavy petroleum feedstock: review. Petrochemistry. 2015, 55 (4), pp. 267-290
13. Milordov D.V., Abilova G.R., Mironov N.A., Yakubova S.G., Yakubov M.R. Comparative analysis of the solubility of asphaltene fractions with addition of petroleum vanadyl porphyrins. Petroleum Chemistry. 2022, pp. 240-249
14. Mironov N., Milordov D., Abilova G., Tazeeva E., Yakubova S., Yakubov M. Preparative-scale purification of petroleum vanadyl porphyrins sulfuric-acid-loaded macroporous silica. Journal of Porphyrins and Phthalocyanines. 2020, 24, pp. 528-537
15. Oliveira D.C., Sacco H.C., Nascimento O.R., Lamamoto Y., Ciuffi K.J. Amino-ironporphyrinosilica hybrid materials. Journal of Non-Crystalline Solid**s.** 2001, 284, pp. 27-33
16. Park P.J., Je J.Y., Byun H.G., Moon S.H., Kim S.K. Investigation of the antifungal activity and mechanism of action of LMWS-chitosan. Journal of Microbiology and Biotechnology. 2004, 14, pp. 317-323
17. Petrova L.M., Abbakumova N.A., Foss T.R., Romanov G.V. Structural features of asphaltenes and petroleum resins fractions. Moscow: Neftekhimiya. 2011, pp.262-266
18. Reiss E., Porta G.D., Rosa I. de, Subra P., Letourneur D.J. Supercritical antisolvent micronization of some biopolymers. Journal of Supercritical Fluid**s.** 2000, 18, pp. 239-245
19. Rytting B.M., Singh I.D., Kilpatrick P.K., Harper M.R., Mennito A.S., Zhang Y. Ultrahigh-purityvanadyl petroporphyrins. Energy & Fuels. 2018, 32, pp. 5711-5724
20. Semeikin A.S., Golubchikov O.A., Koifman O.I. Synthesis and application of porphyrins. Izvestiya Vysshikh Uchebnykh Zavedenii. Khimiya i Khimicheskaya Tekhnologiya, 2005, 48, pp. 14-21
21. Senge M.O., Sergeeva N.N., Hale K.J. Classic highlights in porphyrin and porphyrinoid total synthesis and biosynthesis. Chemical Society Reviews. 2021, 50, pp. 730-4789
22. Yao C., Hoang T., Ma S. Biomimetic catalysis of a porous iron-based metal-metalloporphyrin framework. Inorganic Chemistry. 2012, 51 (23), pp. 12600-12602
23. Zhang L., Lu Y., Du Y., Yang P., Wang X. Synthesis and photocatalytic evolution of hydrogen of meso-tetrakis(p-sulfonatophenyl)-porphyrin functionalized platinum nanocomposites. Journal of Porphyrins and Phthalocyanines. 2010, 14, pp.540-546

ISNN: print 2663-7006; online 2709-2666

ASOIU
Azerbaijan State Oil and Industry

AJCN, Vol .7, No.2 , 2025, pp.26-30
https://doi.org/10.32010/AJCN04022025-26

OBTAINING BIOACTIVE COMPOUNDS FROM POMEGRANATE PEEL WASTE

Gunel Amanullayeva [0000-0003-3058-6703]
Department of "Chemistry and technology of inorganic substances"
PhD, associate professor,
Azerbaijan State Oil and Industrial University
gunel.amanullayeva@gmail.com

Abstract: *The research work shows the advantages of recycling pomegranate peels, which are considered environmental waste. The possibility of obtaining valuable bioactive substances from them has been shown. The substances obtained during extraction are biologically active compounds with a wide range of applications. Ethyl acetate, which is widely used in the food industry, was chosen for the extraction process of pomegranate peels. The extraction process was carried out by the Soxhlet method at 60-77℃. After removing the solvent from the obtained extract, a dark brown resin was obtained. The solubility of pomegranate peel in ethyl acetate was 64.7% according to the results. The main purpose of this work is to identify the functional groups belonging to the bioactive compounds in the composition of the ethyl extract of pomegranate peel. The ethyl acetate extract of pomegranate peel was studied using an IR-FURYE spectrometer. In the spectrum, 4 peaks corresponding to the wavelength of the aliphatic CH bond in alkyl groups were observed in the region of 2984.41 - 2878.28 cm^{-1}. The absorption band at 1738.58 cm^{-1} was attributed to the broad OH group in carboxylic acids.*
Keywords: *biomass, recycling, pomegranate peel, extraction, ethyl acetate, IR spectra.*

INTRODUCTION

Azerbaijan is rich in various types of pomegranate fruit. In recent years, pomegranate production has increased slightly in line with demand. While pomegranate production was 3 million tons in 2018, this figure increased to 4.8 million tons in 2020. Considering the volume of pomegranate production and its juice processing, 500 thousand tons of solid waste are generated worldwide annually. Pomegranate peel and seeds constitute approximately 54% of the fruit and are discarded as waste after the pomegranate is squeezed. Pomegranate fruit waste is considered food waste [1, 2]. Pomegranate fruit consists of 43% peel, 11% seeds, and 46% juice [3]. Pomegranate peel is rich in polyphenols, and polyphenols are cancer-preventing agents, which explains the pharmacological ability of pomegranate [4]. Literature shows that the peel contains more bioactive compounds than other parts of the fruit [5-7].

All parts of the pomegranate have been used as a medicinal product since ancient times. Modern scientific research has revealed that pomegranate has antioxidant, anti-inflammatory, antitumor, immunomodulatory, antibacterial, antiviral, hypoglycemic, antiphrastic, detoxifying, wound healing and other beneficial properties [8]. These beneficial properties are associated with the unique chemical composition of various parts of the plant. The juice and pulp of pomegranate fruit contain up to 20% sugars, organic acids, up to 6% citric and malic acid. Pomegranate juice is rich in Mn, P, Mg, Si, Cr, Ca, Cu salts, vitamins C, B1, B2, B6, B15 [9,10]. The juice of wild and sour pomegranate varieties has a lower sugar content, and an acid content of more than 10%. Pomegranate juice also contains up to 2% proteins, amino acids, up to 12% starch, up to 22% cellulose, polysaccharides and anthocyanins [11, 12]. Pomegranate peel contains

ISNN: print 2663-7006; online 2709-2666

high amounts of carbohydrates (59.60%), moisture (5.40–5.95%), protein (4.90–8.97%), ash (3.40–4.22%), fiber (16.30–19.41%) and fat (0.85%) [13].

Flavonoids, especially catechins, epicatechins, quercetin, anthocyanin, and procyanidins, are the main bioactive components of pomegranate peel. According to studies, the flavonoid content in pomegranate peel is approximately 12.4 times that of juice and seedstimes higher [14, 15]. There has been an increased interest in the synthesis of polymers based on natural and renewable raw materials. According to estimates, the depletion of oil reserves has increased interest in alternative sources. It is known that 5-hydroxymethylfurfural (5-HMF) and its derivatives are used in the synthesis of polymers. In the synthesis of many polymers, polysaccharides, vegetable oils, terpenes, furan-containing derivatives, etc. have been used from various natural macromolecules and renewable monomers [16-18].

It has been used to extract 5-HMF from pomegranate peel and study its physical and chemical properties using modern methods [19].

The presented work deals with the extraction of various bioactive compounds as a result of recycling waste from pomegranate juice production. The composition and structure of the extraction products obtained from the waste of the pomegranate juice production plant are shown using modern analysis methods. The results of the studies on the functional groups, element atoms, and molecular structures in their composition are given.

EXPERIMENTAL PART

An extraction method was used to recycle waste from pomegranate juice production and obtain various bioactive compounds. Ethyl acetate was used as the extractant. The solvent from the extraction process was fractionated by distillation at boiling temperature. The physical and chemical characteristics of the solvent used were - ρ= 0.9003 g/cm^3, nd^{20} = 1.3723, $T_{boil.}$ = 77.1°C, $T_{mel.}$ = -83.6°C, $T_{ign.}$ = -4°C. The pomegranate peels used as the starting material were washed and dried. They were ground into powder in a grinder (fig.1). The powdered form of the pomegranate was analyzed by XRD

Extraction process 60-77°C for 8 hours in a Soxlet apparatus. 13 grams of pomegranate peel and 260 ml of ethyl acetate were used during the process. According to the results, the amount of soluble substance was 64.7%, and the amount of remaining residue was 35.2%.

Fig. 1 Used as raw materials

IR spectra of the used pomegranate peel and its extracted products were recorded at the Institute of Petrochemical Processes. These samples were recorded on an IR-

ISNN: print 2663-7006; online 2709-2666

FURYE spectrometer. The IR-FURYE spectrometer is made in Germany and records in the wavelength range of 400 - 4000 cm^{-1}. It is a Bruker FTIR brand ALPHA Spectral ATR module and its dimensions (WxDxH) are 220 x 330 x 260 mm.

The absorption of infrared radiation at a specific wavelength by each substance provides information about its chemical structure. This method has identified the main functional groups in the extracts, thus clarifying the chemical properties of the bioactive components.

RESULTS AND DISCUSSION

The XRD spectrum of the pomegranate used during the experiment is shown in figure 2. The pomegranate peel powder used was amorphous (fig.2).

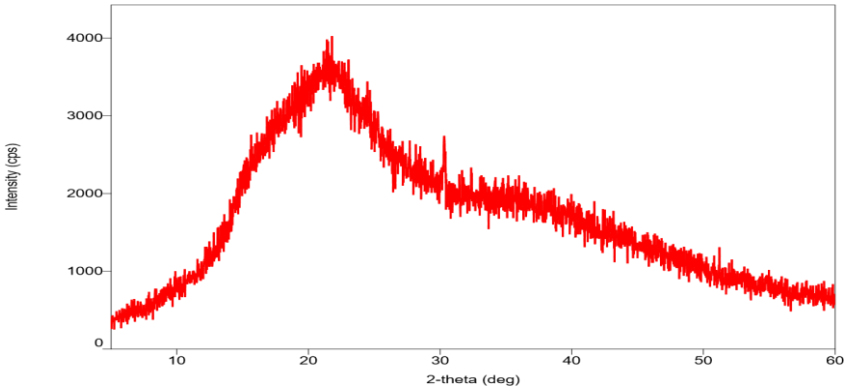

Fig. 2 XRD spectrum of pomegranate peel

The spectra of the ethyl acetate extract of pomegranate peel were recorded using an IR-FURYE spectrometer. The functional groups belonging to the bioactive compounds in its composition were identified (fig.3).

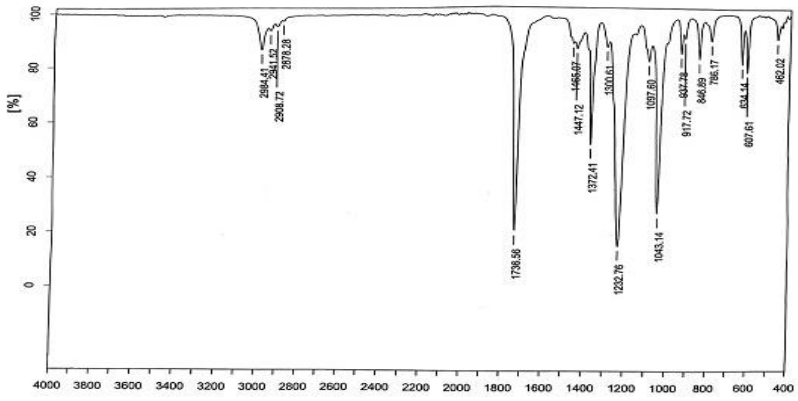

Fig. 3 IR spectrum of ethyl acetate extract of pomegranate peel extract sm^{-1}

In the spectrum, 4 peaks corresponding to the wavelength of aliphatic CH bonds in alkyl groups were observed in the region of 2984.41 - 2878.28 cm^{-1} [20, 21]. The absorption band of the C=C-C aromatic bond was observed in the region of 1466 - 444 cm^{-1} and the absorption corresponding to the CO bond was observed in the region of 1372 - 1043 cm^{-1} [22]. Accordingly, the absorption corresponding to the C=C-C

aromatic bond in the pomegranate peel extract was 1466.07 cm^{-1}, 1447.12 cm^{-1} and the absorption corresponding to the CO bond was 1372.41 cm^{-1}, 1300.61 cm^{-1}. The absorption band of 1738.58 cm^{-1} was found to be present in carboxylic acids.It has been attributed to the broad OH group.

CONCLUSION

The extraction process of pomegranate peel, which is a suitable raw material, was carried out. The main functional groups in the extract were studied by IR spectroscopy. In the ethyl acetate extract of pomegranate peel, an absorption corresponding to the C=C-C aromatic bond was observed at 1646.94 cm^{-1}. At the same time, absorption corresponding to the CO bond was observed at 1372.41 cm^{-1}, 1300.61 cm^{-1} and a broad OH group band in carboxylic acids was observed at 1738.58 cm^{-1}.

REFERENCES

1. Garcia Garcia G., Woolley, E., & Rahimifard S. A framework for a more efficient approach to food waste management. Int. J. Food Eng. 2025, Vol.1(1), pp.65–72. doi: 10.18178/ijfe.1.1.65-72
2. Sagar N.A., Pareek S., Sharma, S., Yahia E.M., & Lobo M.G. Fruit and vegetable waste: Bioactive compounds, their extraction, and possible utilization. Comprehensive Reviews in Food Science and Food Safety. 2018, Vol.17 (3), pp.512–531. https://doi.org/10.1111/1541-4337.12330
3. Ko K., Dadmohammadi Y., & Abbaspourrad A. Bioactives from food and cosmetic byproducts: Pomegranate peel. Bakhis Food. 2021, Vol.10 (3), pp.657. https://doi.org/10.3390/foods10030657
4. Aghahuseynova M.M., Huseynli H.H., Amanullayeva G.İ. Extraction method of obtaining polyphenolic compounds from pomegranate peels. PPOR. Vol. 26, №. 4, 2025, pp.1118-1124. DOI:10.62972/1726-4685.2025.4.1118
5. Rahnemoon, P., Gharachorloo, M., & Bakhshabadi, H. Antioxidant activity and total phenolic content of pomegranate peel extracts in relation to extraction methods and solvent types. Journal of Food Science and Technology. 2016, Vol. 53(1), pp.149–154.https://doi.org/10.1007/s13197-015-1973-8
6. Ullah R., Nadeem M., & Imran M. Extraction and characterization of pomegranate (Punica granatum L.) peel oil. Pakistan Journal of Nutrition. 2012, Vol.11(5), 424–429.https://doi.org/10.3923/pjn.2012.424.429
7. Wang Z., Pan Z., Ma H., & Atungulu G.G. Phenolics extracts from pomegranate peel. Ajigida Scientific Journal. 2011, Vol.5, pp.17–25. https://doi.org/10.2174/18745264101105010017
8. Mphahlele R.R, Fawole O.A., Makunga N.P., & Opara U.L. Effect of drying on the bioactive compounds, antioxidant, antibacterial and antityrosinase activities of pomegranate peel. BMC Complementary and Alternative Medicine. 2016, 16:143, pp.7-12. https://doi.org/10.1186/s12906-016-1054-2
9. Naseem A., Hafsa Z., Nisar Ah., Khalid H. Nutritional quality evaluation of different varieties of pomegranate under climatic conditions of Faisalabad. Eurasian J.Soil Sci. 2019, 8 (2), pp.184–188. https://dergipark.org.tr/tr/download/article-file/693139

ISNN: print 2663-7006; online 2709-2666

10. Dumlu M.U., Gürkan E. Elemental and nutritional analysis of Punica granatum from Turkey. J. Med. Food. 2007, Jun., 10(2), pp.392–395. DOI: 10.1089/jmf.2006.295
11. Muhammad N., Muhammad J.J., Ishtiaq A., Maryam, Irfan A. et all. Biochemical Analysis of Organic Acids and Soluble Sugars in Wild and Cultivated Pomegranate Germplasm Based in Pakistan Plants. 2020, 9, 493, pp.2-14. doi:10.3390/plants9040493
12. Xueqing Zhao and Zhaohe Yuan. Anthocyanins from Pomegranate (Punica granatum L.) and Their Role in Antioxidant Capacities in Vitro. Chem. Biodiversity. 2021, 18(10), e2100399 DOI:10.1002/cbdv.202100399
13. Kandylis P., & Kokkinomagoulos E. Food applications and potential health benefits of pomegranate and its derivatives. Foods. 2020, 9(2), pp.122. https://doi.org/10.3390/foods9020122
14. Kalaycıoğlu Z., & Erim F.B. Determination of antioxidant and antimicrobial properties of pomegranate peel extract. International Journal of Food Science & Technology. 2017, Vol.52(1), pp. 1–8. https://doi.org/10.1111/ijfs.13360
15. Abid M., Yaich H., Cheikhrouhou S., Khemakhem I., Bouaziz M., Attia H., & Ayadi, M. A Selected Tunisian pomegranate peels: LC–MS/MS antioxidant phenolic profiling. Journal of Food Science and Technology. 2017, 54(9), pp.2890–2901.DOI:10.1007/s13197-017-2727-0
16. Coline V., Sylvain C., Nilakshi V. Sadavarte, Bhausaheb V. Tawade, Bernard Boutevin and Prakash P. Wadgaonkar Functionalization of cardanol: towards biobased polymers and additives. Polym.Chem., 2014, № 5, pp.3142-3162. https://pubs.rsc.org/en/content/articlelanding/2014/py/c3py01194a
17. Maxence F., Emilie D., Vincent B., Rémi A., Sylvain Caillol and Bernard Boutevina.Vanillin, a promising biobased building-block for monomer synthesis. Green Chemistry. 2014, Vol. 16, pp. 1987-1998. https://doi.org/10.1039/C3GC42613K
18. Perry A. Wilbon, Fuxiang Chu, Chuanbing Tang. Progress in Renewable Polymers from Natural Terpenes, Terpenoids, and Rosin. Macromolecular rapid communications,. 2013, Vol. 34 (1), pp. 8-37 https://doi.org/10.1002/marc.201200513
19. Amanullayeva G.I., Aghahuseynova M.M. Production of 5-hydroxymethylfurfural based on accessible natural raw materials. PPOR, Special issue. 2025, pp. 147-152. https://doi.org/10.62972/1726-4685.si2025.1.147
20. Hashem A., Chukwunonso O.A., Mohamed F.N, Ashraf A. Efficacy of treated sodium alginate and activated carbon fiber for Pb (II) adsorption. International Journal of Biological Macromolecules. 2021, Vol. 176, No. 15, pp. 201-216 DOI:10.1016/j.ijbiomac.2021.02.067
21. Grassel FS et al. Development of methodology for identification of the nature of the polyphenolic extracts by FTIR associated with multivariate analysis. Spectrochimica Acta Part A: Molecular and Biomolecular Spectroscopy .2016, Vol. 153, pp. 94–101. DOI:10.1016/j.saa.2015.08.020
22. Beltran J., Sanchez-Martin J., Martin-Garcia L. Multiparameter quantitative optimization in the synthesis of a novel coagulant derived from tannin extracts for water treatment. Water Air Soil Pollut. 2012, Vol.223, pp.2277-2286. DOI:10.1007/s11270-011-1022-3

ASOIU
Azerbaijan State Oil and Industry University

AJCN, Vol .7, No.2 , 2025, pp.31-37
https://doi.org/10.32010/AJCN04022025-31

ACCUMULATION OF ORGANOMETALLIC COMPOUNDS ON THE ZCC SURFACE UNDER CONDITIONS OF CATALYTIC OXYCRACKING

[1]*Elvira Guseinova* [0000-0003-0297-1516]
Department of "Petrochemical technology and industrial ecology"
Professor, doctor of chemical sciences,
Azerbaijan State Oil and Industrial University
elvira_huseynova@mail.ru
[2]*Samira Safarova*[0000-0003-4663-5557]
Research Institute "Geotechnological Problems of Oil, Gas and Chemistry
PhD student
ssafarova22@gmail.com
[3]*Maya Abdullayeva* [0000-0002-1380-1216]
Department of "Petrochemical technology and industrial ecology"
Associate professor, Azerbaijan State Oil and Industrial University
mayaabdullayeva@hotmail.com
[4]*Gakhraman Hasanov* [0000-0001-9272-6084]
[4]*Research Institute "Geotechnological Problems of Oil, Gas and Chemistry"*
Professor, doctor of technical sciences
gaman51@mail.ru

Abstract:*The paper presents the results of studying the accumulation of organometallic compounds on the surface of a zeolite-containing catalyst (ZCC) during the catalytic oxycracking of heavy hydrocarbon raw materials. The aim of the study was to determine the nature and degree of accumulation of trace elements that can affect the activity and stability of the catalyst. The experiments were carried out at a temperature of 500 °C, an oxygen concentration of 1 %, a contact time of 1.2-2 s, and a process duration of 900 s. The elemental composition of the catalyst surface before and after catalysis was studied by energy-dispersive microanalysis (EDM). It is established that during the process, the accumulation of trace elements Fe, Ni, Cr, and Ca occurs on the surface of the catalyst Ca, due to their migration from the raw material. As the contact time increases, the Fe content increases to 2.3%, Cr to 0.1%, Ni to 0.04%, and Ca to 0.02 %. The obtained values are significantly lower than the known critical levels at which the active sites of the catalyst are deactivated. This allows us to conclude that the accumulation of metals on the surface of ZCCs is not the main reason for the decrease in its activity during catalytic oxycracking, and decontamination is associated with other factors that require further study.*
Keywords: *catalytic oxycracking, zeolite-containing catalyst, organometallic compounds, energy dispersion analysis, iron, nickel, chromium, calcium, catalyst deactivation.*

INTRODUCTION

Heterogeneous catalysts allow efficient use of scarce raw materials, both renewable (for example, biomass, polymer waste and household waste) and non-renewable (for example, crude oil, coal and natural gas), in a variety of hydrocarbon and carbohydrate conversion processes. Although the popular definition of catalysts suggests that they are not used in the chemical reaction itself, this does not mean that the catalysts have eternal life. Unfortunately, in fact, various chemical and physical processes most often lead to deactivation of solid catalysts. Examples of such processes

ISNN: print 2663-7006; online 2709-2666

are loss of function due to sintering and poisoning of metal, as well as structural degradation processes such as dealuminization of zeolite and destruction of the zeolite framework [1-5]. Another example of catalyst deactivation is the formation of carbon deposits that clog the pores of the catalyst or otherwise prevent access to the catalytic centers. Thus, catalyst decontamination is an important area of both academic and industrial research. The mechanisms of deactivation of new or industrial catalysts are studied both *in in situ* and *operando*. The fact that catalysts are usually deactivated over time makes it difficult to determine the appropriate time in the life of the catalyst to determine activity (or speed (TOF)).

One of the urgent problems of developing the concept of catalytic oxycracking in the presence of ZCC is understanding the dynamics of its activity and selectivity. It is reliably proved that the process parameters have different effects on its selectivity and conversion of VG. In our previous works [6-8], based on the study of the parameters of the catalytic oxycracking process in the presence of ZCCs of the system, it was shown that the temperature and degree of oxidation equally strongly determine the conversion of raw materials and the distribution of products, while the temperature and contact time show the opposite effect. Similar to traditional catalytic cracking (CC), the key parameters are the process temperature and the contact time of raw materials with the catalyst, but their action is multidirectional.

The effect of temperature can be illustrated as follows:

- at 450 °C, the conversion rate reached 54.7 %, the yield of liquid target products was 29.6 %, and that of gaseous products was 16.1 %,
- when the temperature was increased to 500 ° C, the degree of transformation increased to 69.4 %, the yield of light fractions increased to 38.6 %, gas — to 17.3 %, and compaction products (CP) - to 13.2 %. This indicates a simultaneous acceleration of primary and secondary reactions,
- at 550 °C, the conversion reached a maximum of 71.8 %, but the yield of light fractions decreased (to 21.4 %, which is 8% and 17% less than at 500 °C and 450 °C). Gaseous products increased more than twofold due tore-cracking, while coking decreased from 13.2 % to 12.1 %.

In the course of studies on the effect of the duration of the OCC process, the maximum gas yield (35.1 %) was observed after 300 s, and for target liquid fractions I and II - after 600-900 s (up to 38.5–38.6 %). With a further increase in the duration to 1800-2700 s, the conversion decreased to 56.5-55.1 %, which is explained by the accumulation of products of oxidative compaction and blocking of the active centers of the catalyst.

The study of the effect of the oxidation state allowed us to establish that with 0.5% oxygen, the conversion was minimal (36.0 %) at lowcoking, at 1% the conversion increased to 69.0 %, and the total yield of light fractions reached 38.6 %, which is 15.6% higher than with OTC, and only 1.4 % lower than with at 2 %, the conversion was maximal (74.0 %), but the yield of light fractions dropped to 19.7 %. The amount of gas and products of oxidative compaction increased almost exponentially. The unsteady nature of the catalytic oxycracking process was also noted due to the oscillatory deactivation of the catalyst, which is followed by a period of activity.

The marked decrease in the activity of the catalyst can occur due to the formation of coke on the surface, which blocks the active centers. In addition, decontamination can be caused by agglomeration of metals, the action of catalytic poisons entering the

system, changes in the texture and phase composition under the influence of high temperatures. When decontaminated with compaction products or temporary poisons, the activity can be restored by performing appropriate procedures, while in other cases, decontamination is irreversible and requires periodic replacement of the catalyst with a fresh one.

EXPERIMENTAL PART

In the course of the study, 2 types of spent catalyst samples were selected: after catalysis - participation in OCC, and after participation in CC. They were granules with a diameter of 1-2 mm, differed in dark color, and contained individual granules from dark gray to black.

Catalytic experiments were performed in a flow-through installation at atmospheric pressure. A steam-drop mixture of raw materials and oxygen was passed at a linear rate of 1 ml / min through a quartz glass reactor with a diameter of 2 c mind a length of 8 cm, into which 5 cm^3 of the corresponding zeolite was preloaded in the form of granules with a diameter of 1-2 mm. Before feeding the reaction mixture, the catalyst was calcined in a dried air current at 500°C for 2 hours, then the reactor was brought to the required temperature of the experiment in the He current and kept for 10 minutes. The temperature in the reactor was 500°C. In the case of OCC, the oxidation state of raw materials was 1%, and the contact time, equal to the ratio of the catalyst volume (cm^3) to the flow rate of the raw mixture (cm^3/s), was 1.7 s. In the case of CC, all parameters remained unchanged except for the presence of an oxidizer.

The elemental composition was determined by energy-dispersion microanalysis (EDM) on a JEOL JSM-6610 LV electron microscope equipped with a set-top box.

RESULTS AND DISCUSSION

The spent catalyst samples were pellets with a diameter of 1-2 mm. They were characterized by a dark color, and contained individual granules from dark gray to black. The samples that took part in the OCC under mild conditions had a brownish-brown color. This section presents analytical data on the accumulation of organometallic compounds on the ZCC surface.

As is known, the composition of oil includes many metals, including alkaline and alkaline earth (Li, Na, K, Ba, Ca, Sr, Mg), metals of the copper subgroup (Cu, Ag, Au), zinc subgroups (Zn, Cd, Hg), boron subgroups (B, Al, Ga, In, Tl), vanadium subgroups (V, Nb, Ta), many metals of variable valence (Ni, Fe, Mo, Co, W, Cr, Mn, Sn, etc.), as well as typical nonmetals (Si, P, As, Cl, Br, I etc.).

The negligible concentrations of these elements do not allow, given the current state of analytical technology, to isolate and identify the substances in which they are included. It is generally accepted that the elements contained in micro-quantities in oil can be found in it in the form of fine aqueous solutions of salts, fine suspensions of mineral rocks, as well as in the form of complex or molecular compounds chemically related to organic substances. The latter, according to V.F.Kamyanov, are divided into: organoelement compounds, i.e. containing a carbon-element bond; salts of metals substituting for a proton in acidic functional groups; chelates, i.e. intramolecular complexes of metals; complexes of several homogeneous or mixed ligands; complexes with heteroatoms or a π-system of polyaromatic asphaltene structures [9].

ISNN: print 2663-7006; online 2709-2666

In the 70s, research on the composition and physicochemical characteristics of trace elements was intensified in all oil regions of our country – Azerbaijan, D. I. Zulfugarli [10-12]. He summarized the extensive data on the content and distribution of trace elements in oil and sedimentary rocks, organisms and reservoir waters published in the world literature before 1957, including the results of original studies of Azerbaijan's inorganic objects obtained by the author himself.

A great deal of work on the study of trace elements in the oils of offshore fields of Azerbaijan, accompanying and seawater, and the establishment of the relationship of trace elements in them was carried out by Corresponding Member of the National Academy of Sciences of Azerbaijan, Doctor of Chemical Sciences F.Samedova [13]. It was found that the dominant elements in the studied oils are Mn, Mo, Fe (content 91.54-221.7, 313.3-624.4 and 49.7-373.4 g/t, respectively). The studied oils are young and slightly metamorphosed, they are located at depths of 100-4235 m and, apparently, in this connection, they are characterized by a high content of manganese. Compared to the ancient oils of the Mesozoic deposits of the CIS countries, the studied oils of Azerbaijan contain 2-3 orders of magnitude less zinc (0.001-0.007 wt %). According to data from [14], vanadium in the form of pentoxide is contained in oils $4 \cdot 10^{-5}$-$5 \cdot 10^{-5}$ %, traces of nickel in the form of oxide.

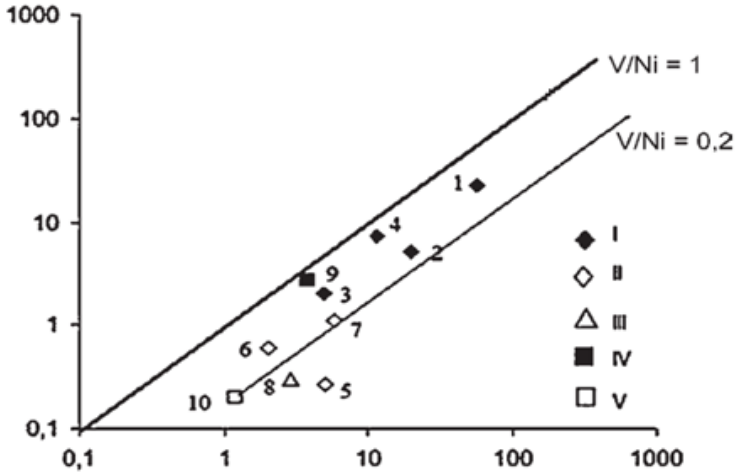

Fig. 1. The ratio of vanadium and nickel in oils generated by OM of rocks of various lithophage. Facies oils: marine: I – deep – water, II-shallow-water; continental: III-lacustrine, IV-coal-bearing with a high content of resinite, V-coal-bearing with a high content of leuptinite. Regions: 1-California; 2-Belarus; 3-Sakhalin; 4-Japan; 5-Azerbaijan; 6-Georgia; 7-Ciscaucasia; 8-China; 9 – Western Siberia (Cenomanian); 10 – New Zealand

According to [15], Azerbaijani oils belong to immature oils of the early generation of the nickel metallogeny, are depleted in ME and formed in immature source rocks. The distribution of Ni in oil fractions confirms its primacy, its association with nitrogenous ligands, and explains the nickel specialization of immature fluids. The transition from fluids generated by OM of marine origin to oils from continental OM (fig.1) results in a decrease in the V and Ni contents. Oil is concentrated in the V/Ni ratio field below unity. Characteristic indicators for Azerbaijani oils are $\sum(V+Ni) \leq 10$,

vanadylporphyrin ∑ V_pVp = 1.7, nickel Ni porphyrin Ni_p = 3 g / t; concentration series, metallogeny - Ni > Fe (V) > V (Fe) Nickel, Ni, Fe, Cu, Pb, Zn, Br, Co, V, As, Au, Ce; Physical and chemical properties-p = 0.850, S (sulfur content,%) = 0.5, C+A (sum of resins and asphaltenes,%) = 12; Type of oil in terms of ME concentration - Depleted (primary).

Table 1

Distribution of metals in fractions

Fraction, °C	Content, 10^{-6} wt%						
	V	Ni	Cu	Fe	Mg	Mn	Ca
250-350	0.007	-	0,30	0,49	0,17	0.003	0.02
350-450	0.025	0.006	10.57	2,54	1,54	0.006	0.35
>450	57.04	24.08	9.12	3.43	4.86	0.009	1.94

As can be seen from the data presented in the table 1, metals in terms of their content in high-boiling fractions are arranged in a row: for the 250-350°C fraction: Fe > Cu > Mg > Ca > V > Ni, Mn; for the 350-450°C fraction: Cu > Fe > Mg > Ca > V > Mn > Ni; for fractions >450°C: V > Ni > Cu > Mg > Fe > Ca > Mn.

The presented results indicate that trace elements in fractions above 350°C can be divided into two groups: vanadium, nickel (as the main ones) and those that are an order of magnitude lower – copper, iron, magnesium and calcium.

It is known that during the processing of heavy raw materials, nickel, iron, copper, cobalt and vanadium compounds poison and destroy the catalyst. Metals are deposited on the cracking catalyst and increase the formation of hydrogen and coke. Since the formation of hydrogen and / or coke usually has a negative effect on the production of target products, both hydrogen and coke are undesirable products of the cracking process. In addition, metals are not removed during the catalyst regeneration process. According to the effectiveness of reducing the activity of ZCCs, they can be arranged in a row: Pb < Cr < Fe<V< Mo < Cu < Co <Ni.

Taking into account the well-known fact that the presence of metals of the first group leads to a decrease in the catalytic activity of ZCCs under cracking conditions, it was of undoubted interest to find out how much the decrease in activity, deactivation of ZCCs under catalytic oxycracking conditions is associated with this factor. Taking into account that in the course of our research, we found that the minimum conversion value was recorded during OCC under conditions of 500°C, 1%, a process duration of 900 s, and a contact time of 2 s, the elemental composition of the spent sample was studied under these conditions. The initial ZCC and post-catalysis ZCCs were also studied as controls under conditions of 500°C, 1%, and a process duration of 900 s, but a contact time of 1.2 s.

The results of our EDM analysis are presented in the form of a graphical relationship (fig 2). It shows the dynamics of both aluminum, silicon, and oxygen, its modifier chlorine, as well as natural aluminum silicate impurities in the form of iron and titanium, and those that appear on the surface of the catalyst after participation in the process of chromium, nickel and calcium. As can be seen from these data, an increase in the contact time from 1.2 to 2 s leads to an increase in the iron content by 0.78-2.29%, chromium by 0.1% by weight, nickel by 0.04% by weight, and calcium by 0.02% by weight. The presence of chlorine on spent catalysts was not observed, which indicates its entrainment during the process.

ISNN: print 2663-7006; online 2709-2666

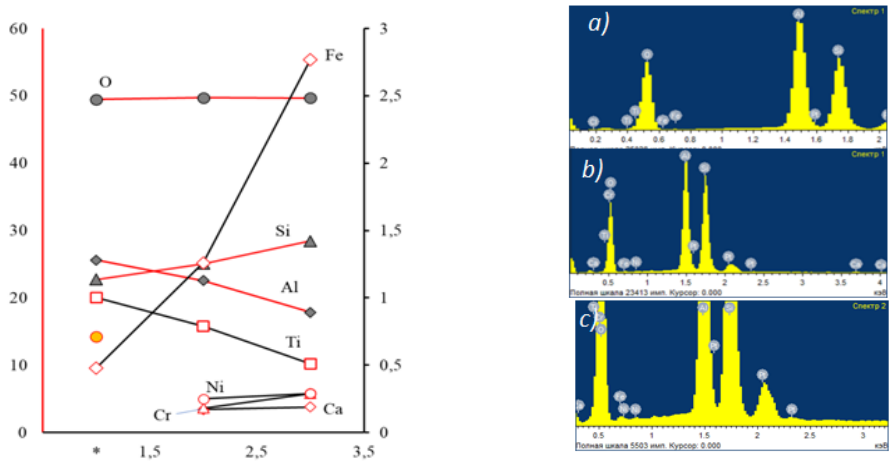

Fig. 2. Dependence of the trace element content and EDM spectra of ZCC samples on the contacttime: a-initial, before catalysis; b – contact time 1.7 s; c – contact time 2 s; * - initial ZCC, before catalysis

Relative to nickel, it enters the raw material in the form of metal porphyrins, etc. complexes. During the cracking process, they are destroyed and Ni is deposited on the surface of the catalyst. Probably, under the conditions of oxidative cracking in the regeneration zone, Ni passes into NiO, interacts with oxygen, and then is reduced again by hydrocarbons in the reactor. As a result, the catalyst is enriched with active Ni^{2+}/Ni^{0} centers, which are not acidic centers of zeolite, but work as dehydrating/dehydrogenating centers of oxidative dehydrogenation. The same can be said about iron. Although it is less active in the dehydrogenation reaction than nickel, its presence nevertheless leads to an increase in the gas and gas yield. Here you should pay attention to one nuance – iron, unlike nickel, chromium, is present in the composition of the initial ZCC (before catalysis). This indicates that its initial concentration is related to the substances used in the preparation of the catalyst. The subsequent increase in its concentration (excluding its ingress due to abrasive wear of the surface of the iron reactor, etc.) is associated exclusively with ingress from raw materials. The increase in conversion in the presence of nickel- ZCC was noted earlier [6,7]. The presence of chromium and calcium is secondary to the activity of cracking catalysts.

At the same time, based on the values known in the literature, at which the critical content of nickel is 2000-3000 ppm, which is 3 times higher than that observed at the contact time of 2 s of the OCC sample, and for iron its "activity" is more than 4 times lower than that of nickel, the obtained values allow us to exclude the fact that accumulation of metals on the surface of the OCC catalyst as the most likely cause of its deactivation.

CONCLUSION

Thus, the energy dispersion microanalysis of the surface of the zeolite-containing catalyst (ZCC) after participation in the catalytic oxycracking process revealed the accumulation of trace elements Fe, Ni, Cr and Ca. It was found that an increase in the contact time of the raw material with the catalyst from 1.2 s to 2 s leads to an increase in

the content of Fe (up to 2.3%), Cr (up to 0.1%), Ni (up to 0.04%) and Ca (up to 0.02%) on the surface of the ZCC. The data obtained indicate the dependence of the degree of metal enrichment on the duration of the interaction of the raw material with the catalyst, which confirms their migration from the feedstock. A comparison of the obtained metal concentrations with the literature data showed that their level is significantly lower than the critical limits at which deactivation of the catalyst surface is observed. This eliminates the accumulation of metals as the main cause of ZCC deactivation during catalytic oxycracking.

REFERENCES

1. Rosyadi, I., Suyitno, S., Arifin, Z., Sutardi, T. Novel approaches to zeolite deactivation mitigation and regeneration in biomass gasification. Journal of Thermal Engineering. 2025, Vol.11(5), pp. 1552-1584
2. Ihli J, Jacob RR, Holler M, Guizar-Sicairos M, Diaz A, Da Silva JC, et al. A three-dimensional view of structural changes caused by deactivation of fluid catalytic cracking catalysts. Nat Commun. 2017, Vol.8(1), 809 p
3. Liu P, Chen Z, Li X, Chen W, Li Y, Sun T, et al. Enhanced degradation of VOCs from biomass gas-ification catalyzed by Ni/HZSM-5 series catalyst. J Environ Manage 2023, 345 p
4. Morales–Leal FJ, Ancheyta J, Torres–Mancera P, Alonso F. Experimental methodologies to perform accelerated deactivation studies of hydrotreating catalysts. Fuel. 2023, Vol.332, 12607 p
5. Das S, Pérez-Ramírez J, Gong J, Dewangan N, Hidajat K, Gates BC, et al. Core–shell structured catalysts for thermocatalytic, photocatalytic, and electrocatalytic conversion of CO_2. Chem Soc Re. 2020 , Vol.49, pp. 2937-3000
6. Guseinova, E.A., Rasulov, S.R. Hydrocarbon Group Composition of the Liquid Products of the Catalytic Oxycracking of Vacuum Gas Oil. Chem Technol Fuels Oils. 2025, Vol. 61, pp. 631 - 634
7. Guseinova, E.A., Rasulov, S.R. Catalytic Oxycracking of Vacuum Gas Oil. Chem Technol Fuels Oils. 2024, Vol.60, pp. 239–243
8. Guseinova, E.A., Adzhamov, K.Y., Mursalova, L.A. et al. Formation kinetics of hydrocarbon compounds in the vacuum gas oil oxycracking process. Reac Kinet Mech Cat. 2020, Vol.131, pp. 57–74
9. Heteroatomic components of oils: a monograph V. F. Kamyanov. Novosibirsk: Siberian Branch, 1983, 236 p
10. Babayev F.R., Martynova G.S., Nanadzhanova R.G. Microelement indication oil of Azerbaijan READINGS OF A.I. BULATOV Materials of I International scientific and practical conference (on March 31). 2017, pp. 97-101
11. Zulfugarli D. I. Copper in the oil of Azerbaijan. -Dokl.AN Az.SSR. 1949, Vol. 5, Sh 12, pp. 492-497
12. Zulfugarli D. I. On the presence of nickel in the oil of Azerbaijan. -Dokl. AN Az. SSR, 1950, Vol. 6, №. 3, pp. 117-123
13. Samedova F. I. Oil of Azerbaijan. Baku, ElmPubl., 2011, 412 p.
14. Masagutov P. M. Alumosilicate catalysts and changes in properties in the cracking of petroleum products. M., Chemistry. 1975, 272 p
15. Punanova S.A. Trace elements in naphthides in oil and gas basins. Doklady Earth Sciences. 2019. Vol. 488. №. 2. pp. 1207-1210

ISNN: print 2663-7006; online 2709-2666

ASOIU
Azerbaijan State Oil and Industry

AJCN, Vol .7, No.2 , 2025, pp.38-43
https://doi.org/10.32010/AJCN04022025-38

INVESTIGATION OF THE AFFECT OF CATALYST ADDITIVE ON CATALYTIC CRACKING PROCESS

[1]*Gulshan Dadayeva*[0009-0002-5097-7015]
Department of "Petrochemical technology and industrial ecology"
Associate Professor, PhD in technical sciences,
Azerbaijan State Oil and Industrial University
gulshan.dadayeva@asoiu.edu.az
[2]*Zuleykha Asgarova*
Department of "Petrochemical technology and industrial ecology"
master's student,
Azerbaijan State Oil and Industrial University
zaskerova25@gmail.com
[3]*Elchin Mammadov*
Department of "Petrochemical technology and industrial ecology"
master's student,
Azerbaijan State Oil and Industrial University
elchin.mammadov000@gmail.com

Abstract: *The study of using non-traditional feedstock resources for the catalytic cracking process enables the processing of a wide range of raw materials, as well as the possibility of regulating selectivity toward various feedstocks. In this regard, the introduction of a Mo catalyst additive—prepared by mixing paramolybdate solution (PMS) with an activating ammonium sulfide solution—into the selected feedstock for the catalytic cracking process leads to the formation of molybdenum disulfide (MoS_2), which is a conventional hydrotreating catalyst component under cracking conditions. This compound exhibits catalytic activity in hydrogenation and hydrocracking reactions. In the presence of the additive, the optimal process conditions correspond to a temperature of 500 °C and an additive concentration of 0.05 wt%. The introduction of the catalyst additive into the feedstock increases the overall acidity of the catalyst from 23.6 to 47.2 µmol during cracking. Moreover, the acidity level of the catalyst and the ratio of acid sites of different strengths intensify the cracking of the feedstock, thereby facilitating the effective progression of reactions during the process.*
Keywords: *Pyrolysis gas, catalytic cracking, Mo catalyst additive, light gas oil fraction, regeneration, vacuum distillate.*

INTRODUCTION

To meet the current demand for engine fuels, expanding oil production volumes has nearly exhausted the available oil refining capacities. To address this issue, increasing fuel resources through deeper and chemically enhanced oil processing, improving the quality of engine fuels, and incorporating alternative fuels into refining processes have become areas of significant interest [1–3].

In the deep processing of petroleum residues, the development and implementation of flexible technological schemes, as well as high-intensity, environmentally benign thermocatalytic and hydrogenation processes, continue to maintain their relevance [4–6].

In this context, the catalytic cracking process plays a particularly important role in the deep refining of oil for the production of engine fuels. This process enables the efficient conversion of easily accessible and heavy feedstocks into high-quality motor gasoline components. At the same time, the process also yields gas components rich in

propane–propylene and butane–butylene fractions, which supply the petrochemical industry. The light gas oil fraction obtained from catalytic cracking is used as a component of diesel fuel and for producing naphthalene, whereas the heavy gas oil is considered a high-quality feedstock for the production of premium “needle-like” coke [7-10].

Taking the above-mentioned factors into account, continuous research has been conducted to intensify the catalytic cracking process. Studies related to exploring new feedstocks for the catalytic cracking process and increasing product yields are considered highly relevant in the field of petrochemistry from both theoretical and practical perspectives [11,12]. In this regard, the aim of the presented scientific study is to investigate the main regularities of catalytic cracking of hydrotreated vacuum distillate in the presence of an additive prepared from a mixture of Mo catalyst precursor—paramolybdate solution (PMS)—with an activating ammonium sulfide solution, intended for the synthesis of molybdenum disulfide, as well as to study its effect on the yield of gases released during the process.

To achieve the desired result, it was necessary to solve the following tasks:

• To study the characteristics of the catalytic cracking process and the composition of the resulting products depending on the type and amount of the PMS additive;

• To determine the optimal conditions of the catalytic cracking process using the PMS additive.

EXPERIMENTAL PART

In the process, vacuum distillate obtained from mixed crude oils processed at the Baku Oil Refinery—specifically from the operating EÜDS and AVQ units—was used as the feedstock. The physicochemical properties of the selected vacuum distillate are presented in table 1.

As an additive, a Mo-containing catalyst precursor was employed, prepared by mixing a paramolybdate solution with an activating ammonium sulfide solution. For preparation, a paramolybdate solution (PMS) dissolved in 20 mL of distilled water was combined with the activating ammonium sulfide solution. The concentration of paramolybdate in the resulting mixture was 3%. The prepared additive was introduced into the vacuum distillate at a concentration of 0.01–0.05 wt% (calculated as Mo), after which the mixture was dispersed in a laboratory mixer at a rotational speed of 5000 rpm for 5 minutes. Prior to mixing, the feedstock was thermostated at 60 °C.

Analytical methods: – The fractional composition of the feedstock and reaction products was determined by gas chromatography using a “Kristallyuks-4000M” chromatograph equipped with a flame-ionization detector, in accordance with ASTM D2887.

– Analysis of the feedstock was performed by thermogravimetric analysis using a “TGA/DSC1 METTLER TOLEDO” instrument.

– Particle size distribution of the dispersed phase in feedstock samples prepared with Mo-containing additives was measured by laser light scattering using an “N5 Submicron Particle Size Analyzer” (Beckman Coulter).

– The composition of liquid products was analyzed using a Thermo Focus DSQ II gas chromatography–mass spectrometry (GC-MS) system.

– The molybdenum content in catalyst samples was determined by atomic absorption spectroscopy (AAS).

ISNN: print 2663-7006; online 2709-2666

Table 1

Physicochemical properties of vacuum distillate

№	Density,kg/m^3	Sulfur amount, Ppm	Cetane number	Fraction content, ^{0}C
1	923	2400	26,8	10% - 238 50% - 272 90% - 318

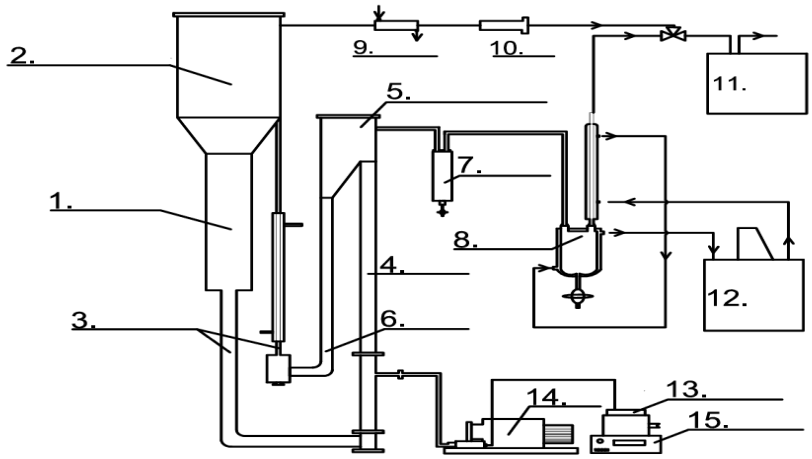

Fig 1. Laboratory equipment of catalytic cracking process: 1-regenerator; 2-separator; 3-transportation line; 4- reactor; 5- separator; 6- desorber; 7-slime settling container; 9-cooler; 10- filter; 11- gas chromatogram ; 12- termostat; 13- vessel; 14- liquid pump; 15-electronic scale

RESULTS AND DISCUSSION

The influence of the feedstock and the molybdenum catalyst additive (PMS) on the cracking process (fig.1) was investigated in a laboratory setup within the temperature range of 480–520 °C. The concentration of the molybdenum-containing additive (PMS) was 0.05 wt%, and the feed rate was maintained at 2 h^{-1}. It was determined that both the pure vacuum distillate used as feedstock and the added PMS exert a measurable effect on the cracking performance parameters depending on temperature. Furthermore, the addition of PMS to the vacuum distillate resulted in a decrease in the average particle size of the dispersed phase compared with the initial vacuum gas oil (320 nm), yielding a particle size distribution in the range of 150–180 nm. The obtained emulsion remained stable for several hours without phase separation, indicating that PMS was uniformly distributed within the feedstock. Thus, once the prepared feed enters the reactor, molybdenum sulfide formed from the decomposition of the additive is evenly dispersed throughout the reactor volume.At process temperatures of 480 and 520 °C, the gasoline yield in cracking runs with and without PMS (fig. 2) was nearly identical; however, at 520 °C, the gasoline yield in the PMS-assisted cracking process (37%) was significantly lower than that in the process without the additive, where it reached 40.0 wt%. In both cases, the conversion of the feedstock remained nearly the same and did not change significantly within the investigated temperature interval, remaining within 90–92.7%. The yield of light gas oil increased

slightly with increasing temperature, and in the PMS-modified feedstock, the light gas oil yield at certain temperatures was lower than that observed in the cracking of the pure feedstock (fig. 3).In the cracking of pure distillate, increasing the temperature from 480 to 520 °C resulted in an increase in the light gas oil yield from 16.0–16.1% to 16.7–16.8%. In the cracking of the feedstock containing PMS, the light gas oil yield under the same temperature conditions increased from 15.2% to 15.6–15.7 wt%.

The yield of gaseous products increases with rising temperature in both cases—cracking with PMS and without PMS. In the cracking of the pure feedstock, the gas yield increases from 20.6–20.8% to 26.1–26.6% as the temperature rises from 480 to 520 °C (fig. 4). It is assumed that, at elevated temperatures, the intensification of cracking reactions of unsaturated hydrocarbons leads to the increased formation of gaseous fractions.

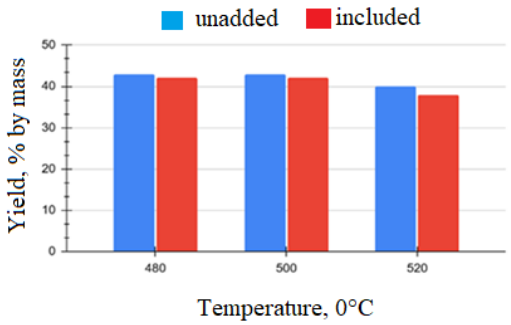

Fig.2. Temperature dependence of gasoline yield

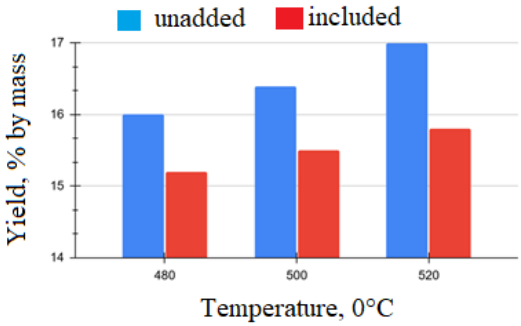

Fig. 3. Temperature dependence of light gas oil yield

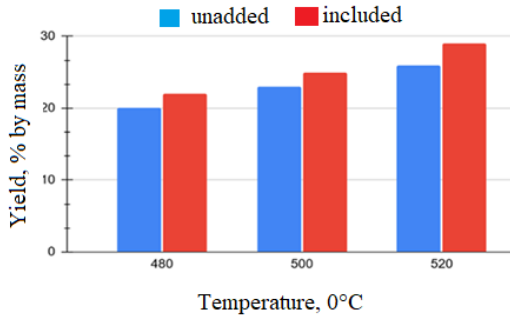

Fig.4. Temperature dependence of cracking gaz yield

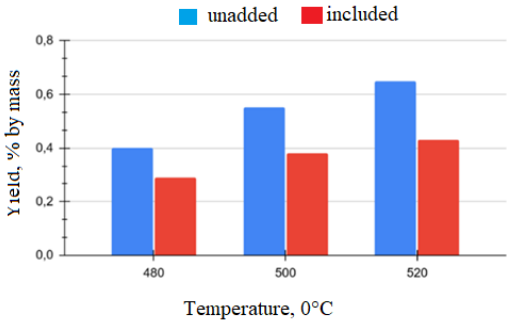

Fig. 5. Temperature dependence of hydrogen yield

A decrease in the hydrogen yield within the gaseous products was observed when PMM was introduced into the process (fig. 5). This indicates an intensification of hydrogenation reactions, which proceed with hydrogen consumption. At the same time, during the cracking of the feedstock in the presence of PMS, hydrogen loss varies depending on temperature. At 480 °C, hydrogen loss is 26%, at 500 °C it increases to 38%, and at 520 °C it reaches 42%. Based on these results, the optimal technological parameters for the catalytic cracking of vacuum distillate with PMS were

ISNN: print 2663-7006; online 2709-2666

determined to be a temperature of 500 °C and a PMS concentration of 0.05 wt% in the feedstock.

CONCLUSION

- The effect of introducing an additive (PMS)—prepared by mixing a paramolybdate solution with an activating ammonium sulfide solution—into the catalytic cracking feedstock (vacuum distillate) in liquid form was investigated.
- The influence of molybdenum-containing additives on product yield, the hydrocarbon composition of the products, and the acidic properties of the catalyst was examined. It was established that the introduction of PMS into hydrotreated vacuum distillate intensifies hydrogenation reactions of hydrocarbons. This is attributed to an increase in the acidity of the active sites of the molybdenum catalyst from 23.6 to 47.2 μmol, thereby promoting a more intensive progression of the reactions.
- It is assumed that the preliminary mixing of PMS with vacuum distillate at a concentration of 0.05 wt% leads to a decrease in the amount of H_2 in the gaseous products at 500 °C. It is believed that a portion of the hydrogen is consumed through the enhancement of hydrogenation reactions during the process.

REFERENCES

1. BP Statistical Review of World Energy. Review statistical review of world energy workbook.xlsx. Christof Rühl, London. 2013, №8, pp. 16
2. Tago T., Konno H., Sakamoto M, Nakasaka ,. Masuda T. Selective synthesis for light olefins from acetone over ZSM-5 zeolites with nano- and macro-crystal sizes. 2011, №183-191, pp. 367-398
3. Khadjiev S.N.,. Gerzeliev I.M., Kapustin V.M, Kadiyev Kh.M., Dementiev K.I. Pakhmanov. O.A. Catalytic Cracking as Part of Modern Deep Oil Refining Complexes. – *Petrochemistry.* 2011, Vol.51, № 1, pp. 33–39
4. PIRAs World Refinery Data Portal Brochure, July 13. 2013, №5, pp. 8-12
5. Vinvenzo Calemma, Roberto Giardino, Marco Ferrari. Upgrading of LCOby partial hydrogenation of aromatics and ring opening of naphtenes over bi-functional catalysts. Fuel Processing Technology. 2010, №9, pp. 770-776
6. MA H.,Hu R., Langan L/, Hunt D., Cheng W.-C., Maximizing FCC Light Cycle Oil by Heavy Cycle Oil Recycle. In: Advances in Fluid Catalytic Cracking. Testing, Characterization, and Environmental Regulations. Ed. by Mario L. Ocelli. CRC Press. 2010, №9, pp. 14-23
7. Chemsystems POPS Executive Report. Global Commercial Analysis: Polyolefins, 2013, pp. 67-83
8. Sheptenko R. D. Technical Zeolites and Technologies for Catalytic Cracking to Light Olefins. Scientific Journal of Toraygyrov University. 2024, №1, pp. 7-19
9. Jun L,. Wei L,. Zhonghong Q,. Huiping T,. Yuxia Z. Catalyst CGP-1 for MlPProcess to Increase. Cleaner Gasoline. In: Studies in Surface Science and Catalysis. Vol.166, № 55, Ed. by M.L. Occelli. Elsevier B.V. 2007, № 34, pp. 14-25
10. Marcilla A,. Hernarndez del Remedio M,. Garcira A.N.. Degradation of LDPE/VGO mixtures to fuels using a FCC equilibrium catalyst in a sand

fluidized bed reactor. Applied Catalysis A. 2008, pp. 256-261
11. Huan W-C,. Huang M-S,. Huang C-F,. Chen C-C,. Ou K.-L. Thermochrmical conversion of polymer wastes into hydrocarbon fuels over various fluidizing cracking catalysts. 2010, № 2305-231 6, pp. 12-28
12. Pakhmanova O.A., Antonov S.V., Dementyev K.I., Gerzeliev I.M. Co-processing of polymer waste and petroleum feedstock in the catalytic cracking process. Abstracts of the IV Russian Conference "Current Issues of Petrochemistry". Zvenigorod. 2012 pp. 215-253
13. Skibitskaya N.A., Yakovleva O.P. Prospects for the Development of Matrix Oil Resources. Drilling and Oil. 2011, № 6, pp. 32-46
14. Myshov A.N. Features of catalytic cracking of oil. International Scientific Journal Bulletin of Science". 2023, Vol.2, № 2 pp. 15-27

ISNN: print 2663-7006; online 2709-2666

ASOIU
Azerbaijan State Oil and Industry University

AJCN, Vol 7, No.2 , 2025 pp.44-51
https://doi.org/10.32010/AJCN04022025-44

INFLUENCE OF THE BINDER TYPE AND QUANTITY ON PHYSICAL, MECHANICAL AND THERMAL PROPERTIES OF SHALE WASTE BRIQUETTES

Elvira Guseinova [0000-0003-0297-1516]
Department of «Petrochemical technology and industrial ecology»
Professor, doctor of chemical sciences,
Azerbaijan State Oil and Industrial University
elvira_huseynova@mail.ru
elvira.huseynova2@asoiu.edu.az

Abstract*: This study investigates the influence of different binding agents—petroleum pitch, coal tar pitch, and bitumen BND 50/70—on the physicomechanical and thermotechnical properties of shale briquettes produced from fine shale fractions. The results demonstrate that the nature and amount of the binder play a decisive role in the formation of the structural framework, mechanical strength, thermal stability, and energy efficiency of the briquetted fuel. The increase in binder content from 5 to 15 wt.% leads to a consistent rise in density, compressive strength, and calorific value, alongside a decrease in porosity, water absorption, and ash content. Coal tar pitch was found to be the most effective binder, providing the highest mechanical strength (3.0–5.5 MPa), lowest water absorption (8–16%), reduced abrasiveness, and the maximum lower heating value (11.2–13.4 MJ/kg). Its high aromaticity and tendency toward carbonization contribute to the formation of a dense coke residue, ensuring long-lasting and stable combustion. Petroleum pitch exhibited moderate performance in both mechanical and thermotechnical parameters and can serve as a balanced and economically feasible binding agent. Bitumen BND 50/70 resulted in briquettes with the lowest strength, highest porosity and water absorption, and the least stable combustion behavior due to its high volatile content and limited carbonization capability. The obtained results confirm a strong correlation between the chemical nature of the binder, its thermal decomposition behavior, and the resulting performance characteristics of shale briquettes. These findings allow for the targeted optimization of briquette formulations depending on their intended application—ranging from high-strength, thermally stable industrial fuel to low-cost, rapidly igniting briquettes for domestic use.*

Keywords. *shale briquettes; binder; petroleum pitch; coal tar pitch; bitumen BND 50/70; physicomechanical properties; thermotechnical characteristics; thermal stability; energy efficiency; briquette structure.*

INTRODUCTION

In recent years, against the background of the global energy transition, increasing demand for resources and the need to diversify sources of carbon raw materials, there has been a growing interest in technologies for processing unconventional energy resources,in particular, shale. According to the data of geological exploration carried out by the State Committee for the Use of the Subsoil of Azerbaijan and confirmed by a number of scientific publications, the total reserves of oil shale in the country are estimated at about 18-20 million tons, while the main deposits are concentrated in the areas of Guba, Dzhangychai and Diyally [1-3]. Despite this, industrial development of these resources remains limited, due to both technological and environmental factors.

Oil shale is a type of solid fossil fuel containing a significant amount of organic matter-kerogen, which can be converted into liquid, gaseous and solid hydrocarbon products under thermal influence. Due to its wide distribution, including on the territory of Azerbaijan, oil shale is considered as an alternative and affordable raw material for the fuel and energy and chemical industries [4-6].

One of the most promising areas is their thermal decomposition (pyrolysis, semi-coking, hydro-pyrolysis, etc.), which results in the formation of liquid hydrocarbons suitable for the production of fuel, bituminous materials and resinous components, as well as gaseous products and solid residues potentially applicable in power engineering and construction.

Along with this, thermal processing of oil shale is accompanied by emissions of harmful substances, including nitrogen oxides, sulfur dioxide, phenols and polycyclic aromatic hydrocarbons. For example, when processing 1 million tons of shale in chamber furnaces, the emission of nitrogen oxides can reach 7 tons per year, and when burning shale in power plants-up to 500 tons [7,8]. In addition, increased concentrations of phenols and other toxic compounds are observed in the wastewater of oil shale processing plants [9].

The legislative framework of Azerbaijan in the field of energy and environmental protection provides for the regulation of activities related to the extraction and processing of energy resources. The Law of the Republic of Azerbaijan "On Energy" defines the basic principles and requirements for energy activities, including the need to comply with environmental standards [10] In this regard, the relevance of the research aimed at developing environmentally friendly technologies for thermal processing of oil shale and efficient use of the resulting products is obvious. This will not only expand the country's raw material base, but also minimize the negative impact on the environment, contributing to the sustainable development of Azerbaijan's energy sector.

The aim of the study was to determine the effect of the type and amount of organic binders (oil pitch, coal pitch, and BND 50/70 bitumen) on the physical, mechanical, and thermal properties of shale fines briquettes.

EXPERIMENTAL PART

Based on the results of previous studies, the object of this research is selected oil shales from the Iyimishly field (Azerbaijan) - typicalallagite shales with a high kerogen content [11,12]. Their shale fines up to 6 mm in size were used for briquetting. Petroleum and coal tar pitch, as well as petroleum road bitumen BND 50/70, were used as binders (table 1) in the amount of 5-15% by weight.

The composition was briquetted on a laboratory hydraulic press PGL-20 at a pressure of 10 MPa without wetting. Determination of the strength characteristics of the obtained shale briquettes was carried out according to the standard method (GOST 21289-75) "Coal briquettes. Methods for determining mechanical strength". The briquette was placed between the cylindrical inserts of the press so that the inserts rested against the centers of its parallel surface, and brought it to destruction. Since oil shales contain up to 50% mineral impurities, which leads to an increase in the strength of briquettes, the number of discharges was increased from 4 (according to GOST 21289-75) to the number leading to complete destruction of briquettes. The thermal stability of shale briquettes (they do not collapse during heat treatment) was determined at a temperature of 800-1000 °C in a muffle furnace.

ISNN: print 2663-7006; online 2709-2666

Table 1

Physical and mechanical characteristics of binders

Parameters	Petroleum pitch	Coal pitch	Bitumen BND 50/70
Density, kg/ m^3	1054	1264	984
Penetration at 25°C, mm	17	1,8	65
Extensibility at 25°C, cm	6	0	144
Cohesion at 25°C, N/m^2	$(1,62)\cdot10^6$	$(2,3)\cdot10^5$	-
Softening temperature, °C	74	87	48
Meltingpoint, °C	101	108	-
Extremely broken structure, °C	184	186	-
Flashpoint, °C	218	232	320
Viscosity, Pa · s at 100°C	576	343	361
at 200°C	0.9	0.6	0.4

RESULTS AND DISCUSSION

According to literature data, the extraction and processing of oil shale forms from 30 to 40% of shale fines, which, except for burning at thermal power plants, does not find industrial use and accumulates in significant quantities on stacks. At the same time, when producing shale gas in gas generators, up to 12% of heavy high-resinous resin is obtained. In addition, shale processing is accompanied by the formation of ash (up to 50% of the initial mass of oil shale).

The data presented in table 2 allow us to estimate the influence of the binder type (petroleum pitch, coal pitch, BND 50/70 bitumen) and its content (5, 10 and 15 %) on the main physical and mechanical properties of shale briquettes. In all three cases, an increase in the proportion of binder leads to an increase in density, which is associated with an improvement in the compaction of the grain structure and the filling of pores with an organic component. Coal tar pitch is characterized by maximum density values (1180-1260 kg / m^3), which reflects its ability to form the most solid carbonaceous framework. The BND values of 50/70 are minimal (1120-1170 kg / m^3), which is explained by the lower carbonization and more ductile nature of bitumen. Oil pitch occupies an intermediate position-the density is from 1150 to 1220 kg / m^3.

There is an obvious dependence of the crushing strength - it increases with increasing binder content, but the growth pattern differs for each type: coal pitch is the best reinforcing component (strength: 3.0-5.5 MPa), oil pitch - average efficiency (strength: 2.5-4.5 MPa) and the lowest strength in briquettes with HDPE (strength: 2.0–4.2 MPa).

The impact strength index reflects the ability of the briquette to retain mass under mechanical stress. the best results were obtained for briquettes containing coal tar pitch (85-95 %). It provides the most resistant to destruction of the frame. The indicator was especially low at 5 % BND, which indicates the weakness of the plastic bitumen frame.

The durability of the briquette was evaluated byits abrasionresistance. Minimal abrasion was observed when using coal tar pitch (8-15%), while for BND - maximum, especially when the binder content is low (12-25 %).

Minimal water absorption was provided by the introduction of coal tar pitch (8-16 %), which is most important for storing briquettes. In our opinion, this is due to high hydrophobicity and carbonation. Unlike pitches, bitumen does not create a solid carbon

frame, remains soft and elastic, so it does not completely fill the pores between particles. As a result, the maximumwater absorption of BND is observed (13-22 %).

Table 2

Influence of the binder type and quantity onphysical and mechanical parameters of briquettes

Index	Binder type and quantity		
	5 %	10 %	15 %
Petroleum pitch			
Density, kg / m^3	1150	1200	1220
Compressive strength, MPa	2.5	4.0	4.5
Impact strength, % saved weight	80	90	92
Abrasionresistance, % weight loss	18	12	10
Water absorption in 24 hours, %	18	13	10
Type of compression failure	brittle	transition	visco-viscoelastic
Coal pitch			
Density, kg / m^3	1180	1230	1260
Compressive strength, MPa	3.0	4.8	5.5
Impact strength, % retained weight	85	93	95
Abrasionresistance, % mass loss	15	10	8
Water absorption in 24 hours, %	16	11	8
Type of compression failure	brittle	transition	viscoelastic plastic
BND 50/70			
Density, kg / m^3	1120	1150	1170
Compressive strength, MPa	2,0	3,0	3,8
Impact strength, % saved weight	70	82	88
Abrasionresistance, % weight loss	22	16	12
Water absorption in 24 hours, %	20	18	13
Type of compression failure	Brittle	ductile-brittle	ductile

The structural evolution of the frame as the binder increases for all binders is as follows: brittle → transient → visco-plastic (or ductile). Coal and oil pitch form the most durable and carbonaceous coke frame. While bitumen forms a plastic matrix, it weakly resists destruction.

Thermal engineering indicators are the key characteristics of fuel briquettes, since they determine the energy value, combustion efficiency and the possibility of industrial use of the resulting fuel. Table 3 shows comparative data on the most important heat engineering indicators of briquettes of the studied compositions.

Data analysis shows that an increase in the binder content from 5 to 15 % leads to an increase in both the lowest and highest calorific values in all the systems studied. This is due to an increase in the proportion of the organic component in the briquette structure and a decrease in the relative content of the mineral part. The highest values of calorific value were observed for briquettes on coal-fired pitch (13.4-14.5 MJ / kg), which is explained by the high content of aromatic carbon structures and a high degree

ISNN: print 2663-7006; online 2709-2666

of carbonization of pitch during heating. Petroleum pitch shows moderate values of calorific value, while BND 50/70 bitumen provides the lowest values.

Table 3

Influence of the binder type and quantity on heat engineering parameters of briquettes

Figure	Type and amount of binder		
	5 %	10 %	15 %
Petroleum pitch			
Lower heat of combustion, MJ/kg	10,5	11,5	12,5
Higher heat of combustion, MJ/kg	11,5	12,6	13,6
operating humidity, %	6	5	4
Total ash, %	52	50	48
Content of volatile substances, %	44	46	50
Flash point, °C	430	420	410
Character of combustion	medium with a tendency to agglomerate	more stable uniform	steady, pronounced coke residue
Coal tar pitch			
Lower heat of combustion, MJ/kg	11,2	12,4	13,4
Higher heat of combustion, MJ/kg	12,2	13,5	14,5
operating humidity, %	6	5	4
Total ash, %	51	49	47
Content of volatile substances, %	39	37	35
Flash point, °C	450	440	430
Character of combustion	dense, moderate; tendency to agglomerate	stable, smooth burning; dense coke residue	long burning; pronounced coke residue
BND 50/70			
Lower heat of combustion, MJ/kg	10,8	11,6	12,2
Higher heat of combustion, MJ/kg	11,8	12,7	13,4
operating humidity, %	7	6	5
Total ash, %	53	51	49
Content of volatile substances, %	46	48	50
Flash point, °C	410	400	390
Character of combustion	quick start, a moderate burning	smoother, with the stabilization of combustion	sustained combustion, coke soft phase

The working humidity decreased with increasing binder content, which is explained by an increase in the hydrophobicity of briquettes and a decrease in capillary porosity. However, an important pattern is observed between binders: bitumen briquettes have the highest humidity (7-8 % at 5% of the binder), which is associated with the softness of bitumen and the saturation of the material with open pores,

briquettes on coal pitch are characterized by the lowest real availability of moisture, which confirms a high degree of hydrophobization of the structure.

Ash content is one of the key parameters that determine the energy efficiency of shale briquettes and their behavior during combustion. The mineral part, which is part of shale fines and binders, does not participate in the combustion process, so an increase in its share leads to a decrease in the real calorific value of fuel and an increase in the inertial heat balance. In addition, high ash content contributes to the formation of a significant amount of solid residues, which can lead to slagging of furnace devices, reduce heat exchange and increase operating costs. Theobtained data show that as the binder content increases, the relative ash content decreases, which is associated with an increase in the organic phase and better binding of mineral particles. The lowest ash content values are typical for briquettes in coal-fired pitch, which further explains their higher calorific value and combustion stability. Thus, reducing the ash content is an important criterion for improving the quality of briquettes and is directly related to the effectiveness of the selected binder type. Among the samples under consideration, the ash content naturally decreases with an increase in the proportion of the organic part, while the minimum ash content corresponds to coal pitch (47-53 %), the maximum-to bitumen, which, as noted in table 2 is associated with less completecarbonization and a large relative contribution of the mineral part.

The content of volatile substances is fundamentally different by the type of binder and reflects the thermal decomposition and structure of the organic matrix. Rapid ignition, low ignition temperature and a less stable combustion zone are associated with the maximum volatility of bitumen-containing briquettes (46-52 %). Oil pitch has average volatile values (44-50%), which ensures a more uniform combustion process.

The values of the ignition temperature fully correlate with the content of volatile substances: bitumen - minimum temperatures (390-420 °C), which ensures a quick start of combustion, but leads to instability of the process; oil pitch is characterized by moderate values (410-440 °C), which creates balanced ignition conditions and reproducible combustion mode; coal pitch has the highest ignition temperatures (430-465°C), which is a sign of high temperature resistance and the formation of a strong coke residue.

The nature of combustion also fully confirms this pattern: bitumen provides rapid ignition, but a soft and unstable coke phase; oil pitch provides a transition from moderate to stable combustion with an increase in the binder content; coal pitch forms the longest, stable combustion with a developed strong coke frame.

CONCLUSION

The obtained results on the study of physical, mechanical and thermal characteristics of shale briquettes with various types of binders (oil pitch, coal pitch, BND 50/70) allow us to identify patterns that determine the formation of the structure, strength and energy properties of composite fuel. The comparative analysis shows that the nature and amount of binder have a decisive influence on the macro - and microstructure of briquettes, their performance and thermal behavior during combustion.

First of all, attention is drawn to the steady increase in density and compressive strength with an increase in the amount of binder in all the systems under study. This is explained by the fact that the organic binder phase acts as a structure-forming

ISNN: print 2663-7006; online 2709-2666

component that fills interparticle pores, improving the contact between mineral grains of shale fines and reducing the number of defects in the structure. The most pronounced increase in mechanical strength is typical for briquettes in coal-fired pitch. Its high aromaticity and ability to further polycyclize when heated ensure the formation of a dense carbon frame, which is manifested in the maximum strength values at 10-15 % of the binder. Oil pitch shows intermediate values, while BND 50/70 bitumen forms the most plastic, but less strong structure due to insufficient carbonizing ability and increased residual porosity.

Abrasion and impact strength, which characterize the resistance of briquettes to mechanical influences, also show the advantages of coal pitch. Minimal abrasion values with high impact strength values indicate a strong structural grid and high resistance to destruction. At the same time, bitumen briquettes show the greatest mass loss during abrasion — which is a consequence of the high plasticity of the binder, weak interparticle adhesion and a larger number of open pores. These results confirm a close relationship between the structure of the organic binder, the degree of compaction of the briquette and its resistance to mechanical loads.

Water absorption is an important operational indicator that determines the behavior of fuel during storage and transportation. Analysis of the data shows that briquettes on coal pitches have minimal water absorption, which is due to the high hydrophobicity and low porosity of the carbon frame. Oilfield briquettes show moderate values, while bitumen briquettes show maximum values, which is due to the lower ability of bitumen to compact the structure and the preservation of a significant number of capillary channels. Thus, the water absorption level clearly reflects the structural density and hydrophobicity of the binder, which affect the resistance of briquettes to external moisture.

Thermal engineering indicators also show significant differences depending on the type of binder. In particular, the heat of combustion increases with increasing amount of binder, which is explained by an increase in the proportion of organic phase and a decrease in the relative ash content. Coal tar pitch provides maximum calorific value due to the high concentration of polycyclic aromatic structures that are prone to carbonization, and the formation of a strong coke residue, which contributes to long-term, uniform combustion. Petroleum pitch forms a moderately pronounced coke residue, ensuring stable combustion, while bitumen gives a soft and less stable coke phase, which leads to faster burnout and less stability of the process.

The content of volatile substances plays a key role in the ignition mechanism. Bitumen contains the maximum amount of volatiles (up to 50-52 %), which provides easy ignition, but leads to less thermal stability and rapid burnout. Oil pitch exhibits intermediate values of volatility. The lowest values are typical for coal tar pitch, which corresponds to its high temperature resistance and the need for higher ignition temperatures. Accordingly, the ignition temperature is a reflection of the depth of aromatization of the binder and directly affects the nature of the flame and the thermal mode of combustion.

A combined analysis of thermal engineering and physical and mechanical data allows us to conclude that coal tar pitch is the most effective binder, providing the optimal combination of high strength, low porosity, minimal water absorption and maximum calorific value. Oil pitch forms balanced characteristics and can be considered as a universal option for the production of medium-strength shale briquettes. It is advisable to use BND 50/70 bitumen only if there are no requirements for high

mechanical strength and combustion stability, since it forms the most porous, less strong structure and has limited heat resistance.

Thus, the discussion of the results demonstrates a close relationship between the chemical nature of the binder, its quantitative content, and the totality of thermal and mechanical characteristics of briquettes. The obtained regularities can serve as a basis for optimizing the composition of shale briquettes depending on the intended purpose: from высокотермостойкихhighly heat-resistant fuel forms to cheap and easily flammable briquettes for household needs.

REFERENCES

1. Abbasov O.R., Ibadzade A.J., Mammadova A.N. «Genesis and organic-geochemical characteristics of oil shale in Eastern Azerbaijan». SOCAR Proceedings. 2018, № 3, pp. 004–015
2. Efendieva, Z. J., & Khalifa-zade, Ch. M. Prospects for the use of oil shale in Azerbaijan. Mining Journal. 2020 , №3, pp. 43–49 https://doi.org/10.17580/gzh.2020.03.16
3. Abbasov, O. R. Geological and geochemical properties of oil shale in azerbaijan and petroleum potential of deep-seated eocene-miocene deposits. Journal European Journal of Natural History, 2016, № 2, pp. 31-40. Retrieved from https://world-science.ru/en/article/view?id=33536
4. Kök, M. V., & Pamir, R. Thermal analysis of oil shale pyrolysis. Thermochimica Acta. 2000, 357–358, pp. 75–81
5. Qian, J., & Wang, J. Oil Shale Petroleum Processing. Fuel Processing Technology. 2006, 87(9), pp. 665–673
6. Speight, J. G., & El-Gendy, N. S. Handbook of Oil Shale. Springer. 192 p
7. Environmental impact of oil shale combustion. Fuel Processing Technology. 2012, 85(1–2), pp. 107–118. https://doi.org/10.1016/S0378-3820(03)00109-4
8. Helfrich, W., & Yunker, M. B. Characterization of polycyclic aromatic hydrocarbons released during oil shale processing. Environmental Science & Technology. 1995, 29(10), pp. 2523–2530. https://doi.org/10.1021/es00010a020
9. Dyni, J. R. Environmental issues of oil shale development. U.S. Geological Survey Scientific Investigations Report. 2006, 49 p. https://pubs.usgs.gov/sir/2005/5294/
10. Azerbaijan Republic. Law of the Republic of Azerbaijan on Energy (№. 541-IQ). Adopted on November 24. 1998, Retrieved from https://eqanun.az/framework/3507
11. Adzhamov, K. Y., Rasulov, S. R., Guseinova, E. A., & Gasanova, S. M. Fiziko-khimicheskaya kharakteristika goryuchikh slantsev mestorozhdeniy Dzhangichay, Bolshoy i Maly Siyaki (Respublika Azerbaidzhan) [Physico-chemical characteristics of oil shale deposits Dzhangichay, Bolshoy Siyaki and Maliy Siyaki (Republic of Azerbaijan)]. News of the Ural State Mining University. 2019 3(55), pp. 39–45. https://doi.org/10.21440/2307-2091-2019-3-39-45
12. Guseinova, E. A. and eth. Thermal analysis of oil shale in the Baygushlu and Iyimish fields. Chemical Problems. 2022, 20(4), pp. 341–346 https://doi.org/10.32737/2221-8688-2022-3-341-346

ISNN: print 2663-7006; online 2709-2666

ASOIU
Azerbaijan State Oil and Industry

AJCN, Vol .7, No.2 , 2025, pp.52-56
https://doi.org/10.32010/AJCN04022025-52

DEVELOPMENT OF ANTI-KNOCK ADDITIVES FOR AUTOMOTIVE GASOLINE

[1]*Elshan Zeynalov*[0000-0002-5372-8754]
Department of "Petrochemical Technology and Industrial Ecology"
associate professor, candidate of chemical sciences,
Azerbaijan State Oil and Industrial University
zeynalov.elshan@asoiu.edu.az
[2]*Mahammad.Huseynov*
Department of "Petrochemical Technology and Industrial Ecology"
master, Azerbaijan State Oil and Industrial University

Abstract: *The efficient and reliable operation of modern automobile engines directly depends on the quality of the gasoline used in the fuel system. One of the main technological characteristics of gasoline is its knock resistance, that is, its resistance to self-ignition under high compression ratios. The knock process leads to a decrease in engine power, incomplete combustion of fuel, energy loss, as well as damage to the piston, valves, and cylinder walls. Therefore, the production of gasoline characterized by a high octane number is of special importance for extending the service life of engines and ensuring compliance with environmental regulations. The present study investigated the effect of various oxygenate blends (MTBE and IBA) on the octane number of automotive gasoline. The effectiveness of these oxygenates was increased due to the emergence of a synergistic effect when they were blended. A synergistic effect was observed with the combined action of a two-component mixture of MTBE and IBS in ratios of 20–80 and 80–20 wt.%, respectively, resulting in an increase in the octane number of gasoline fractions to 1.3–2.0 units compared to that of individual oxygenates.*
Keywords : *automotive gasoline, additives, oxygenates, octane number, synergistic effect.*

INTRODUCTION

The modern, intensive development and improvement of equipment that uses petroleum products as fuel places strict demands on their operational and environmental characteristics. Despite an increase in production volume and the expansion of the range of environmentally friendly gasoline, the demand for it is not being fully met today [1-3]. This is because domestic production of components and additives for automotive gasoline does not meet more than half of the total demand. Under conditions of limited imports, ensuring the production of automotive gasoline is of particular importance.

Traditional technologies for producing high-octane gasoline components based on processes (reforming, catalytic cracking, alkylation, isomerization) are basic, but require significant investments for their implementation, and the current pace of construction and modernization of secondary oil refining plants is currently insufficient. Moreover, the inclusion of components obtained as a result of these secondary processes in gasoline increases the content of combustion by-products in the exhaust gases [4].

A promising innovative direction for expanding the raw material base for motor gasoline is the search for new ways to recycle waste and by-products of petrochemistry and oil refining, which are a source of valuable hydrocarbons. Using these technologies to produce new gasoline components will reduce exhaust gas emissions and increase production volumes and product margins [5-7].

It should be noted that the characteristics of gasoline fuels can be improved by using various substances or their mixtures. Additives, detergents, and components are of great importance for improving the operational characteristics of fuels. They improve the fuels' anti-knock properties, suppress the knock process, improve gasoline vaporization, and reduce the amount of harmful substances in exhaust gases [8-10].The purpose of the present study is to investigate the effect of the composition of oxygenates added to automotive gasoline on the increase in its octane number. For this study, we have selected isobutanol (IBA) and methyl tert-butyl ether (MTBE) as the oxygenates.

EXPERIMENTAL PART

In this research work, methyl tert-butyl ether (MTBE), isobutyl alcohol (IBA) and a model fuel mixture (light straight-run gasoline, catalytic cracking gasoline and isomerate) were used as research objects. The study used standard determination methods for the analysis of primary and target products.

In the initial sample and the reaction products, the mass fraction of the components was determined by gas-liquid chromatography on a “Tsvet-800” gas chromatograph with a thermal conductivity detector. The temperature of the detector thermostat was 220°C, the temperature of the column was 110°C, and helium was used as the carrier gas at a flow rate of 50 cm^3/min. A 6 m × 3 mm column was packed with the sorbent. The sorbent was diatomaceous earth impregnated with Triton-100 liquid phase. The mass concentration of the components was calculated by the internal standard method.

The octane number was determined by the Research Method (RM) according to GOST 8226 and by the Engine Method (EM) according to GOST 511, using a standard single-cylinder engine from a WIT-85 type apparatus.

Gas-liquid chromatographic analysis (GLC) of the samples was performed on a SHIMADZU "GC-2014" gas chromatograph using GsBP-1msc capillary columns. Column characteristics: length 30 m and internal diameter 0.25 mm with applied stationary phase 100% dimethylpolysiloxane, column temperature was changed at a rate of 5°C/min from 40 to 300°C, FID detector, temperature on the detector 300°C, evaporator temperature 300°C, carrier gas helium.

RESULTS AND DISCUSSION

The use of oxygenates as additives to improve the properties of automotive gasoline is considered a global trend. It is known that MTBE and butyl alcohols are considered effective oxygenates. MTBE has a low boiling point and a high saturated vapor pressure, which causes it to evaporate during fuel storage in the summer, leading to a loss of knock resistance and a deterioration of the performance characteristics of gasoline. Compared to MTBE, butyl alcohols have several advantages. In particular, they have low vapor pressure and low toxicity, but their production volume is not as high. Although alcohols, as anti-knock additives, meet the environmental requirements for automotive gasoline, the increased alcohol content in gasoline leads to excessive fuel consumption due to their lower heating value (table 1).

In a number of studies [2-4], it has been shown that the effectiveness of these oxygenates can be increased due to the emergence of a synergistic effect during their

ISNN: print 2663-7006; online 2709-2666

mixing. Taking the foregoing into account, iso-butyl alcohol (IBA) and methyl tert-butyl ether (MTBE) were selected by us as the oxygenates for the study.

Individual oxygenate samples and their mixtures were added to the model fuel blend at 10% (w/w). This amount increases the volume of light gasoline fractions, which positively affects the fuel's initial properties. In the two-component mixture, the MTBE/IBA ratio was varied in 10% (w/w) steps. In the resulting fuel compositions, the octane number was measured by engine and research methods, and the increase in ON was calculated (table 2).

Table 1

Main physicochemical properties of MTBE and IBS

№	Indicator names	MTBE	IBA
1	Density at 20°C, kg/m³	746	802
2	Boiling point, °C	55	107.7
3	Octane number by research method	118	108
4	Saturated vapor pressure, kPa, at 38°C	61	8.5
5	Solubility in water, %(w/v)	1.3	8.5
6	Maximum permissible content in gasoline, %(vol.)	15	10
7	Combustion heat, kJ/g	38220	35520
8	Mass fraction of sulfur, mg/kg	110	1

Table 2

Dependence of the increase in the octane number of a model fuel mixture on the composition of a two-component mixture

№	Additive	Increase in octane number	
		By engine method	By research method
1	IBS	5.3	6.9
2	MTBE	5.9	6.2
3	MTBE : IBS = 90 : 10	5.9	6.3
4	MTBE : IBS = 80 : 20	6.0	7.3
5	MTBE : IBS = 70 : 30	6.6	7.6
6	MTBE : IBS = 60 : 40	6.8	7.8
7	MTBE : IBS = 50 : 50	6.9	7.9
8	MTBE : IBS = 40 : 60	6.9	8.0
9	MTBE : IBS = 30 : 70	7.0	8.2
10	MTBE : IBS = 20 : 80	6.6	8.0
11	MTBE : IBS = 10 : 90	5.5	7.0

It has been shown by us that to a model fuel mixture containing 10% (w/w) of MTBE and IBA, in a ratio of 20:80 and 80:20% (w/w), respectively at ratios of 20:80 and 80:20 (by weight) to the model fuel mixture, respectively, the addition of MTBE and IBA blends to the fuel mixture provides a greater increase in octane number compared to the use of individual oxygenates (6.2 and 6.9 for MTBE and IBA, respectively). The addition of MTBE and IBA to the model fuel blend in a two-component mixture at ratios of 20:80 and 80:20% (wt.), respectively, provides a greater increase in the octane number compared to the use of individual oxygenates (6.2 and 6.9

for MTBE and IBA, respectively).The study of the effect of the MTBE/IBA ratio in the two-component mixture on the anti-knock activity of the fuel blend revealed a synergistic effect on the octane number for IBA content in the range from 20% (wt.) to 80% (wt.).

The observed synergistic effect of the binary mixtures under investigation can be explained by the fact that the boiling point and molecular -mass characteristics result in their being drawn into all narrow petrol fractions, which leads to a uniform increase and distribution of knock resistance across all fuel fractions.

Thus, a synergistic effect was observed with the combined action of the two-component mixture of MTBE and IBA at ratios of 20:80 and 80:20%, respectively (w/w) ratio, a synergistic effect was observed, which is manifested by an increase in the octane number of the petrol fractions by 1.3–2.0 units compared to the individual oxygenates.

CONCLUSION

As a result of research into the complementarity and synergism of oxygenates (methyl tert-butyl ether (MTBE) and isobutyl alcohol (IBA)), new components and additives for motor gasolines have been developed using commercially available domestic raw materials.

A synergistic effect was observed with the combined action of a two-component mixture of MTBE and IBS in ratios of 20–80 and 80–20 wt.%, respectively, resulting in an increase in the octane number of gasoline fractions to 1.3–2.0 units compared to that of individual oxygenates.

REFERENCES

1. Chirkova Yu.N., Arkhipov I.V. Modern requirements for motor gasoline [Electronic resource] / Yu.N. Chirkova, I.V.Arkhipov. “Scientific and practical electronic journal Alley of Science”. 2018, № 5 (21), pp. 133-141
2. Ganina A.A. Developing a method for producing a new component of automobile gasolines on the basis of a by-product of petrochemistry. A.A. Ganina, I.E. Kuzora, S.G. Dyachkova, D.A. Dubrovsky, I.A. Semenov. Theoretical Foundations of Chemical Engineering. 2020, Vol. 54, № 4, pp. 452-458
3. Russo M.V. A resource-based perspective on corporate environmental performance and profitability. M.V. Russo, P.A. Fouts Academy of Management Journal. 2017, T. 40, № 3, pp. 534-559
4. Ashrafov R.A. Requirements for modern environmentally friendly high-octane motor gasolines / R.A. Ashrafov, A.S. Kulieva, V.K. Alexandrov. Scientific works of NIPI NEFTEGAZ SOCAR. 2011, № 4. pp. 67-73
5. Andreev D.Y. Effect of intensification of production of petroleum products on production costs and cost reduction. D.Y. Andreev, S.G. Lopatina. Chemistry and technology of fuels and oils. 2012, № 5, pp. 359 – 362
6. Abdulminev K.G. Technologies of Motor Gasolines with Improved Environmental Properties: A Study Guide / K.G. Abdulminev. Ufa: Ufa State Petroleum Technical University Publishing House. 2011, 103 p
7. Vedenkin D.A., Samoshin R.E., Zuev O.Y. Laboratory complex for processing of oily waste using microwave technology. 2015 International Conference on Antenna

ISNN: print 2663-7006; online 2709-2666

Theory and Techniques: Dedicated to 95 Year Jubilee of Prof. Yakov S. Shifrin, ICATT 2015 - Proceedings 10. 2015. pp. 7136898
8. Zeynalov E.T., Javadzada N.N. Ecological problems caused by the formation of toxic compounds during the exploitation of motor fuels and their solution methods. Azerbaijan Journal of Chemical News. 2023, Vol. 5, №2, pp. 75-85
9. Ershov, M.A. Production of Advanced Automotive and Aviation Gasos in Russia / M.A. Ershov, V.E. Yemelyanov. National Oil and Gas Forum. Moscow. 2014, 19 p
10. Wen Yu. Gasoline Blending System Modeling via Static and Dynamic Neural Networks / Yu Wen, America Morales. International Journal of modeling and simulation. 2004, Vol.24, № 3. pp. 151 – 160

ATTENTION FOR AUTHORS!

Journal "Azerbaijan Journal of Chemical News" approved by the Higher Attestation Commission under the President of Azerbaijan Republic and it is included to the list of journals and periodicals that should be published by major scientific results of dissertations in Azerbaijan Republic.